

Electrical Technology and Engineering

An Academic Article



FAKULTI TEKNOLOGI DAN KEJURUTERAAN ELEKTRIK UNIVERSITI TEKNIKAL MALAYSIA MELAKA

Editorial Team

Patron

HIDAYAT ZAINUDDIN

Advisor

GAN CHIN KIM FAIRUL AZHAR ABDUL SHUKOR

Editor-in-Chief

AMINURRASHID NOORDIN

Associate Editor

SUZIANA AHMAD NURUL SYUHADA MOHD SHARI

Editor

MOHD BADRIL NOR SHAH, ZAMANI MD. SANI, MUHAMMAD SHARIL YAHAYA, AZHAN AB RAHMAN, ZULKIFLI IBRAHIM, NUR ILYANA ANWAR APANDI, SYAHRUL HISHAM MOHAMAD @ ABD RAHMAN, MOHD HANIF CHE HASAN, MOHD FARRIZ MD BASAR MOHD RAZALI MOHAMAD SAPIEE, NUR EZYANIE SAFIE.

Guess Editor

MOHD AZLI SALIM AMAR FAIZ ZAINAL ABIDIN

Published and printed in Malaysia by Penerbit UTeM Press Universiti Teknikal Malaysia Melaka Hang Tuah Jaya 76100 Durian Tunggal Melaka, Malaysia

Tel: +606-270 1241 Faxs: +606-270 1038

Preface

All praise is due to Allah, the Most Gracious, the Most Merciful the ultimate source of success for granting us the strength and inspiration to complete this edition of Electrical Technology and Engineering @ e-TechVolt.

First and foremost, my deepest appreciation goes to our gifted writers and contributors. Your insights, creativity, and dedication breathe life into each page of this e-TechVolt. Your passion continues to be the driving force behind our shared vision.

I would also like to extend my heartfelt thanks to our meticulous editorial team. Your unwavering commitment to quality, attention to detail, and pursuit of excellence ensure that every edition upholds the standards our readers have come to expect. Your work is truly commendable.

As we look ahead to the next volume, we remain steadfast in our mission to deliver thought-provoking, engaging, and meaningful content. We sincerely thank you for your continued support and look forward to sharing more knowledge and innovation with you.

Warm regards, Editor-in-Chief

Electrical Techology and Engineering (e-TechVolt) from Fakulti Teknologi dan Kejuruteraan Elektrik, Universiti Teknikal Malaysia Melaka is an academic article publication platform that will publish twice a year.

Table of Contents





SENSOR-INTEGRATED DUST CLEANING MECHANISM USING BLOW AND SUCTION METHOD FOR ENHANCED WIRE BOND PROCESS

1-5



DEVELOPMENT OF STREETLIGHT MAINTENANCE NOTIFICATION VIA GLOBAL SYSTEM FOR MOBILE COMMUNICATIONS (GSM)

6-10



DESIGN AND DEVELOPMENT OF SPHERICAL ROBOT CONTROL BY A SMARTPHONE APPLICATION

11-16



CAMERA AUTO-CALIBRATION USING PARTICLE SWARM OPTIMIZATION

17-20



AUTOMATED PH-CONTROLLED WITH ALARM INTEGRATION FOR WATER TREATMENT SYSTEM

21-26



TEMPERATURE IMPROVEMENT ACCURACY USING RESISTANCE TEMPERATURE DETECTOR (RTD) FOR PRODUCT QUALITY

27-32



DEVELOPMENT OF A TEMPERATURE-CONTROLLED MOTOR STABILIZATION SOLUTION FOR HIGH-SPEED TESTING MACHINES

33-39



SOLAR CHARGING MONITORING SYSTEM USING ARDUINO UNO FOR LIGHTING APPLICATION

40-44

ELECTRICAL TECHNOLOGY AND ENGINEERING

(An Academic Article)



SENSOR-INTEGRATED DUST CLEANING MECHANISM USING BLOW AND SUCTION METHOD FOR ENHANCED WIRE BOND PROCESS

Asri Din^{1,*}, Azmirul Nashmin Hablum¹, Nur Ezyanie Safie¹, Zaihasraf Zakaria¹,
Ahmad Zubir Jamil¹, Parvin Krisnasamy²

¹Faculty of Electrical Technology and Engineering, Universiti Teknikal Malaysia Melaka

²Department of POA WB STS (WIREBOND SPICE), Dominant Opto Technologies Sdn. Bhd. Melaka

*Corresponding author: asridin@utem.edu.my

ABSTRACT

Wire bonding is a critical process in semiconductor packaging that requires a clean surface for reliable electrical connections. Dust contamination on bonding areas can compromise bond integrity, leading to defects, electrical failures, and reduced product quality. This study proposes a sensor-integrated dust removal system that combines real-time detection with a coordinated blow and suction mechanism. The system is designed to activate only when dust is detected, ensuring targeted cleaning, optimized energy usage, and minimal disruption to production flow. Implemented within an industrial wire bonding environment, the prototype system was tested across six product models. Results demonstrated an average defect reduction of over 40%, confirming the system's effectiveness in eliminating dust-related bonding issues. Automation of the cleaning process reduces manual intervention, enhances consistency, and improves overall production yield. The proposed solution shows strong potential for industrial-scale adoption in high-precision, high-volume electronics manufacturing. development will focus on scalability, IoT-based remote monitoring, and adaptive control for optimized performance.

INTRODUCTION

The wire bond process is central to the assembly of semiconductor devices, ensuring electrical connectivity between chips and external components. However, it is highly susceptible to contamination, particularly from microscopic dust particles that compromise adhesion and conductivity, leading to product failure and reliability issues [1]. Despite advances in cleanroom environments, localized dust on bonding surfaces remains a persistent problem.

Conventional cleaning methods such as vacuuming, ultrasonic baths, and plasma treatment are often manual or limited in integration, making them inefficient in high-speed production lines [2]. To address these shortcomings, this research explores an



automated system that uses real-time sensor feedback to detect and eliminate dust particles prior to bonding.

Several studies emphasize the effectiveness of integrating sensor technologies for air quality and particulate monitoring. Foldable-circuit and optoelectronic sensors, for instance, have enabled miniaturized dust detection with real-time precision in IoT and industrial applications [3]. Additionally, image-based and laser-triggered dust sensors have demonstrated success in embedded systems for environmental and semiconductor applications [4][5].

This study proposes an innovative blow and suction mechanism, controlled by photoelectric sensors, to clean bonding surfaces only when dust is detected—minimizing energy use and increasing process reliability. The objective is to validate this system's impact on defect reduction, process efficiency, and potential for industrial deployment.

METHODS

This project was implemented at Dominant Opto Technologies Sdn. Bhd. and involved the development of a prototype cleaning mechanism integrated directly into the wire bonding line.

A. Design and Components

The dust removal system was designed with a focus on automation, responsiveness, and compatibility with industrial wire bonding environments. The core components of the system are integrated to work in synchrony to detect and eliminate dust particles from bonding surfaces before the bonding process begins. A photoelectric sensor (Panasonic) is mounted near the wire bond track to detect the presence of incoming substrates. Upon detection, the sensor triggers the cleaning cycle, ensuring that cleaning is performed only when material is present (see Fig.1a).

To facilitate the cleaning process, a solenoid air valve is employed to control short bursts of compressed air (see Fig.1b), while an inline filter ensures that the air used is clean and free from additional particulates as illustrated in Fig.1c. The entire system is powered and controlled using a 24V DC power supply (see Fig.1d) and relay module, which provides reliable switching and operational logic for the cleaning mechanism as shown in Fig.1e).



(a) Photoelectric sensor



(b) Solenoid air valve



(c) Inline filter









(d) 24v DC power supply

(e) Relay module

(f) Vacuum suction system

Fig 1. Components used in the integrated system

A vacuum suction system is also integrated and positioned opposite the air nozzle to capture dislodged dust particles immediately after they are removed from the surface. This dual-action approach effectively prevents recontamination and maintains a clean bonding area throughout the production cycle (see Fig.1f). Each component was selected based on industrial compatibility, ease of integration, and effectiveness in high-precision manufacturing environments.

B. Operational Setup

The cleaning system was mounted adjacent to the wire bond tool. Upon material detection, the photoelectric sensor triggered an air pulse through a solenoid valve while simultaneously activating the suction mechanism. Fig.2a shows the wire bond machine without the blow and suction system, whereas Fig.2b illustrates the machine after integration of the proposed cleaning mechanism, highlighting the added components and their positioning relative to the bonding area.



(a) Wire bond machine without cleaning system



(b) Wire bond machine with integrated blow and suction mechanism.

Fig 2. Comparison of wire bond machine setup before (a) and after (b) integration of the blow and suction cleaning system. *Courtesy of Dominant Opto Technologies Sdn. Bhd.*



C. Data Collection and Evaluation

Data were collected from six product models over two periods before and after the system was implemented. For each model, defect counts including dents, missing parts, and lead frame issues were recorded. No inferential statistics were used due to the small sample size, but descriptive analysis was conducted to assess improvement.

RESULTS AND DISCUSSION

The comparison of defect data pre- and post-installation across six models is summarized in Table 1.

Table 1. Defect comparison before and after cleaning system implementation across six product models.

Model	Output (unit)	Damage Before (unit)	Damage After (unit)	Reduction (%)
A	5000	150	90	40.0%
В	3000	80	50	37.5%
С	4000	120	65	45.8%
D	6000	180	100	44.4%
E	3500	95	55	42.1%
F	5500	160	85	46.9%

The results indicate a significant improvement in defect rates across all six product models following implementation of the proposed dust removal system. An average defect reduction of 42.8% was recorded, with individual model improvements ranging from 37.5% to 46.9% (Table 1). These figures underscore the effectiveness of integrating sensor-triggered blow and suction mechanisms in reducing particulate-induced failures in high-precision wire bonding processes. The consistent trend across multiple models supports the system's robustness and compatibility with diverse product lines.

These findings are consistent with studies emphasizing the impact of dust on microelectronic reliability and the success of real-time sensor-guided cleaning systems. Recent developments in smart dust sensors and optoelectronic platforms support the effectiveness of sensor-based control in high-precision environments [3][4]. Moreover, laser-enabled sensors and differential pressure-based detection systems are already revolutionizing particle detection in semiconductor lines [5][6].

The study was limited to one industrial setting and descriptive statistics. Future work should include inferential analyses and scale-up testing across varied environments. Integration with IoT dashboards for remote monitoring and adaptive airflow control is also a promising direction.



CONCLUSION

This project successfully developed and implemented a sensor-integrated blow and suction mechanism that significantly reduces defects in wire bonding processes. Realtime dust detection enables precise, targeted cleaning that enhances product quality and minimizes manual rework. With potential for broader application in precision manufacturing, the system offers a scalable solution for automated contamination control in semiconductor assembly lines.

ACKNOWLEDGMENT

The authors would like to express their sincere appreciation to Universiti Teknikal Malaysia Melaka (UTeM) and Dominant Opto Technologies Sdn. Bhd. for their valuable collaboration in the Work-Based Learning (WBL) program under the Bachelor of Technology curriculum. This project was carried out in response to a real industrial challenge identified during the WBL placement, leading to the successful development of an innovative, industry-relevant solution.

CONFLICT OF INTERESTS

None

REFERENCES

- [1] M. N. Ayuni, M. F. Lin, and L. Q. Zhe, "Deep Learning-Based Classification Approach for Wire bonding Defects inspection," IEEE Int. Conf. On Software Engineering and Computer Systems, pp. 286–290, Aug. 2023, doi: 10.1109/icsecs58457.2023.10256336.
- [2] P. Xie, J. Liu, K. Chen, and P. Zhou, "Study on the dust concentration evaluation for submicron semiconductor particles in confined space based on laser transmission," Journal of Nanoelectronics and Optoelectronics, vol. 18, no. 2, pp. 138–148, Feb. 2023, doi: 10.1166/jno.2023.3381.
- [3] C.-Y. You et al., "Foldable-circuit-enabled miniaturized multifunctional sensor for smart digital dust," Chip, vol. 1, no. 4, p. 100034, Nov. 2022, doi: 10.1016/j.chip.2022.100034.
- [4] T. Song and P. Zuo, "Novel Sensor Applied on Dust Measurement for Integrated Circuits," 12th Int. Workshop on EMC of Integrated Circuits, pp. 284–286, Oct. 2019, doi: 10.1109/emccompo.2019.8919848.
- [5] A. Abdulhameed, Y. Mahnashi, M. A. Al-Absi, and Q. Drmosh, "Investigation of Capacitive-Based Dust Sensor with Nanowires Sensing Layer," IEEE Int. Conf. On Electrical and Electronics Engineering, pp. 42–46, Apr. 2024, doi: 10.1109/iceee62185.2024.10779224.
- [6] J. Xie et al., "Dust trajectory sensor: Accuracy and data analysis," Review of Scientific Instruments, vol. 82, no. 10, Oct. 2011, doi: 10.1063/1.3646528.



DEVELOPMENT OF STREETLIGHT MAINTENANCE NOTIFICATION VIA GLOBAL SYSTEM FOR MOBILE COMMUNICATIONS (GSM)

Vigineswaran A/L Chandran¹, Dr. Nur Azura Binti Noor Azhuan¹, Dr. Nur Ezyanie Binti Safie¹, Ts. Dr. Suziana Binti Ahmad¹, Nurul Syuhada binti Mohd Shari^{1,*}

¹Faculty of Electrical Technology and Engineering, Universiti Teknikal Malaysia Melaka

*Corresponding author: nurul.syuhada@utem.edu.my

ABSTRACT

This project focuses on the development of a streetlight maintenance notification system by Global System for Mobile Communications (GSM) technology. Streetlights are crucial in preventing accidents by improving visibility for drivers; however, maintaining them is equally essential. The system uses GSM to collect and transmit data via SMS, automatically detecting streetlight malfunctions and sending alerts to authorities. The absence of streetlights can have various effects. The first effect is a car accident when the streetlight malfunctions. It makes it difficult for everyone. To decrease the statistics of accidents caused by nonfunctioning streetlights and slow repair response times, this project can be helpful.

INTRODUCTION

Streetlight plays a crucial role in ensuring road safety, especially at night, by improving visibility for drivers, pedestrians, and other road users. Although often taken for granted, well-functioning streetlights play a crucial role in reducing the risk of accidents by illuminating traffic signs, road conditions, and potential hazards [1]. The current approach to streetlight maintenance largely relies on manual reporting, often through websites or hotlines. This may result in delayed repairs and increased accident risks, particularly in rural or less monitored areas. This method is inefficient and highly dependent on public awareness and initiative, leading to prolonged repair durations. A proactive and automated system can bridge this gap, ensuring timely detection and maintenance.

This project focuses on developing an automated streetlight maintenance notification system using Global System for Mobile Communications (GSM) technology [2-3]. The proposed system detects streetlight malfunctions through integrated sensors and sends Short Message Service (SMS) alerts, including location data, to the relevant authorities. This real-time notification mechanism can improve maintenance response time and operational efficiency.



METHODS

This study adopts an experimental design focused on the development and evaluation of a streetlight maintenance notification system using Global System for Mobile Communications (GSM). The study involved multiple stages, including component selection, circuit design and simulation, hardware implementation, and performance analysis of the prototype. The aim was to ensure that streetlight malfunctions could be automatically detected and reported via SMS to relevant authorities for immediate response.

The system design comprises input, process, and output stages, where sensors (heat, water level, and light-dependent resistor) serve as inputs and an Arduino Mega 2560 microcontroller acts as the processing unit as shown in Figure 1. Outputs include an LCD, LED indicators, and GSM-based SMS alerts. Circuit functionality was first verified using Proteus simulation before being implemented in hardware. The sensor responses and GSM message delivery were tested repeatedly under controlled conditions to validate real-time performance [4-5].

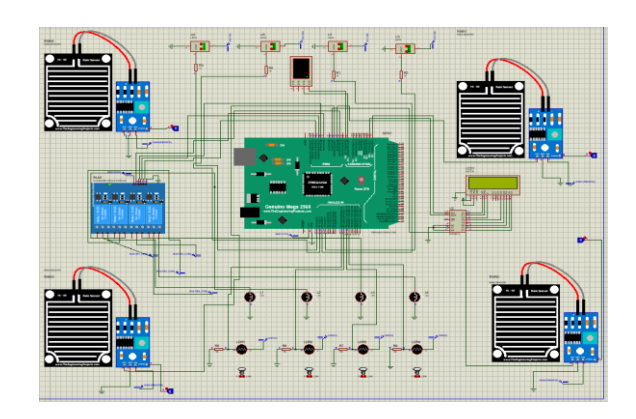


Fig 1. Circuit diagram in proteus software

RESULTS AND DISCUSSION

The findings are categorized based on three fault conditions that are heat, water, and light malfunctions. Each condition was analyzed through simulation in Proteus, and data was collected via sensors interfaced with Arduino Mega 2560.

Case 1: Notification Due to Heat Malfunction

The system was tested using an LM35 temperature sensor. Table 1 presents the temperature readings and the system's response, including light status and SMS notifications. As shown, the system does not trigger alerts at lower temperatures (10–20°C), keeping the lights ON. At 30°C and above, the lights switch OFF, and SMS notifications are triggered, indicating effective heat fault detection as demonstrated figure 2.



Table 1. Output of Temperature Sensor and Notification

Temperature (°)	Light (L1)	SMS
10°	On	No message
20°	On	No message
30°	Off	Yes message
40°	Off	Yes message
50°	Off	Yes message



(a) Lamp 1 malfuntion

Case 2: Notification Due to Water Malfunction

LIGHT 1 FAULTY, Temp=34.56c

(b) SMS notification Fig 2. Lamp 1 heat malfunction

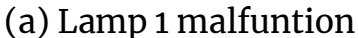
For water detection, a water level sensor simulated flood conditions. As shown in Table 2, the value of '0' represents no water (light ON), and '1' represents water detected (light OFF, SMS will be sent). The system effectively turned off the affected streetlight and sent SMS notifications when flooding occurred, as demonstrated in figure 3.

Table 2. Output of Water Level Sensor

	Light (L4)	SMS
0	On	No message
1	Off	Yes message









(b) display on panel

FLOOD DETECTED!!

(c) SMS notification

Fig 3. Water malfunction

Case 3: Notification Due to Light Malfunction

The Light-Dependent Resistor (LDR) was used to determine if a streetlight failed to emit light at nighttime. The system simulated faulty light behavior, turning OFF when no light was detected and sending SMS alerts.

Table 3. Output of LDR Sensor

LDR	Light 2
0	On
1	Off

CONCLUSION

The development of a GSM-based streetlight maintenance notification system has demonstrated the feasibility and effectiveness of automating streetlight fault detection and notification. By integrating temperature, water level, and light sensors with a microcontroller and a GSM module, the system accurately identified different types of malfunctions and promptly notified the relevant authorities through SMS alerts. This proactive maintenance approach significantly enhances response time, improves public safety, and reduces the risk of accidents particularly in rural or less-monitored areas.

ACKNOWLEDGMENT

The author(s) would like to thank Fakulti Teknologi dan Kejuruteraan Elektrik for the support and resources provided for this research. Appreciation is also extended to all individuals who contributed to the success of this study.

REFERENCES

[1] X. Shen, J. Kong, Y. Song, X. Wang, and G. Mosey, "Optimizing the environmental design and management of public green spaces: Analyzing urban infrastructure and long-term user experience with a focus on streetlight density in the city of Las Vegas, NV," Information Fusion, vol. 118, p. 102914, Jan. 2025, doi: 10.1016/j.inffus.2024.102914. Available: https://doi.org/10.1016/j.inffus.2024.102914



- N. A. A. Rahman et al., "GSM module for wireless radiation monitoring system via SMS," IOP Conference Series Materials Science and Engineering, vol. 298, p. 012040, Jan. 2018, doi: 10.1088/1757-899x/298/1/012040. Available: https://doi.org/10.1088/1757-899x/298/1/012040
- [3] S. Abedi, M. H. Moradi, and R. Shirmohammadi, "Real-time photovoltaic energy assessment using a GSM-based smart monitoring system: Addressing the impact of climate change on solar energy estimation software," Energy Reports, vol. 10, pp. 2361–2373, Sep. 2023, doi: 10.1016/j.egyr.2023.09.038. Available: https://doi.org/10.1016/j.egyr.2023.09.038
- [4] P. Chiradeja and S. Yoomak, "Development of public lighting system with smart lighting control systems and internet of thing (IoT) technologies for smart city," Energy Reports, vol. 10, pp. 3355–3372, Oct. 2023, doi: 10.1016/j.egyr.2023.10.027. Available: https://doi.org/10.1016/j.egyr.2023.10.027
- [5] J. Dixit, Dr. D. Katiyar, and Mr. G. Goel, "AUTOMATIC STREET LIGHT CONTROLLER SYSTEM USING LDR AND PIR SENSOR," journal-article, May 2021. Available: https://ijcrt.org/papers/IJCRT2105743.pdf
- [6] M. Kanthi and R. Dilli, "Smart streetlight system using mobile applications: secured fault detection and diagnosis with optimal powers," Wireless Networks, vol. 29, no. 5, pp. 2015–2028, Feb. 2023, doi: 10.1007/s11276-023-03278-9. Available: https://doi.org/10.1007/s11276-023-03278-9



DESIGN AND DEVELOPMENT OF SPHERICAL ROBOT CONTROL BY A SMARTPHONE APPLICATION

Siti Nor Atirah Binti Samuji¹, Aminurrashid Noordin^{1,*}
¹Faculty of Electrical Technology and Engineering, Universiti Teknikal Malaysia Melaka
*Correspondence: aminurrashid@utem.edu.my

ABSTRACT

This project focused on the design and development of a spherical robot capable of wireless control and terrain navigation through a wheel-driven mechanism. The robot, consisting of two hemispheres, encased a small internal vehicle responsible for locomotion. Its movement was controlled via a smartphone over a Wi-Fi connection and integrated with a Hibiscus Sense board, which included gyroscopes, accelerometers, two A4988 motor drivers, two stepper motors, and a graphical user interface (GUI). The project aimed to investigate the challenges and limitations associated with the robot's drive mechanism, control strategies, and sensing capabilities. Additionally, the robot's performance was evaluated across various surfaces, including tarmac, grass, sand, cement, and carpet. While the spherical robot demonstrated omnidirectional mobility on level ground, it encountered stability issues on uneven or low-friction surfaces such as grass, sand, and tarmac. Overall, this project contributed to the development of a novel spherical robot capable of performing tasks in diverse environments through wireless communication.

INTRODUCTION

A spherical robot is a spherical-shaped mobile platform capable of omnidirectional movement and performing complex tasks such as environmental monitoring and surveillance. These functions can be controlled via smartphone or computer applications. To enhance situational awareness and safety, the integration of an Inertial Measurement Unit (IMU) sensor and a wireless camera is proposed.

Disaster Risk Reduction (DRR) refers to the concept and practice of minimizing disaster risks through systematic efforts to analyze and mitigate the underlying causes of disasters. The objective of DRR is to prevent the emergence of new risks, reduce existing ones, and effectively manage residual risks, all of which contribute to increased resilience and the realization of sustainable development goals. One key application of DRR is the deployment of robots in disaster scenarios, particularly for Search and Rescue (SAR) operations.

SAR robots, as illustrated in Figure 1, are compact and autonomous systems designed to navigate disaster-stricken areas and locate victims without relying on the Global Positioning System (GPS) or wireless communication networks [1]. Disaster response



robots, such as the one shown in Figure 2, feature a hybrid design that enables mobility through three different modes: legged, wheeled, and legged-wheeled configurations [2].



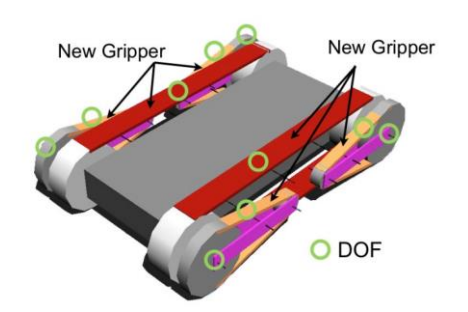
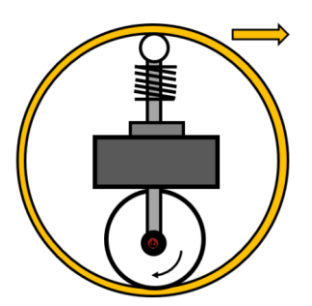
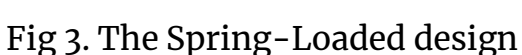


Fig 1. SAR robot for navigation

Fig 2. Disaster robot

The direct-drive method for the locomotion of spherical robots includes non-holonomic drive systems, such as four-wheeled differential mechanisms and spring-loaded internal drive units (IDUs), as illustrated in Fig. 3. Although spring-loaded IDUs are cost-effective, they often suffer from steering instability and slippage. These issues can be mitigated by optimizing the internal tension and surface friction parameters [3]. Furthermore, researchers in [4] developed the BHQ-III robot, which utilizes a dualmotor configuration one motor dedicated to propulsion and the other to controlling the IDU. This design significantly improves holonomic movement and enables more precise turning capabilities.







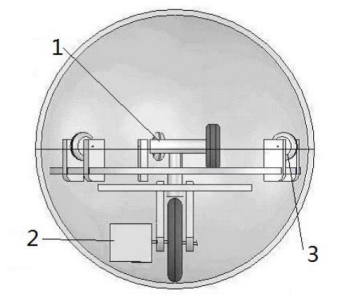
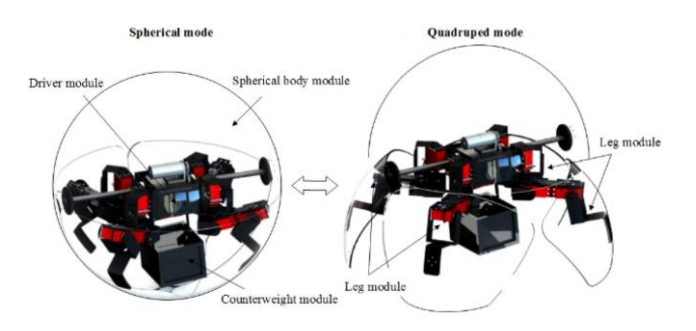


Fig 4. BHQ-III

On the other hand, shape deformation and hybrid locomotion methods have been explored by researchers, where the core concept involves combining spherical structures with bionic limb mechanisms. This integration enables the robot to both roll and walk, as illustrated in Figure 5. Such robots can adapt to diverse terrains by switching between quadrupedal locomotion and energy-efficient spherical rolling modes [5]. Other innovative designs, such as the one shown in Figure 6, incorporate split-shell mechanisms with omnidirectional wheels. These robots achieve directional control through dynamic shape transformation and adjustments to their center of gravity [6].





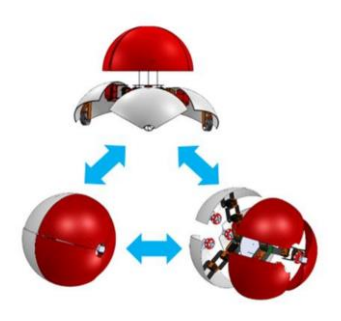


Fig 5. Spherical robot with bionic limb

Fig 6. Seformable shape spherical robot

METHODS

The methodology encompasses two key stages: mechanical design and electronics design.

ROBOT MECHANICAL DESIGN

The spherical robot is enclosed within a durable, translucent acrylic shell, consisting of two identical hemispheres with an outer diameter of 180 mm and an inner diameter of 177 mm. The internal components are strategically arranged, as illustrated in Figure 7. A camera bracket supports a compact HD spy camera $(3.4 \times 3.4 \times 4.5 \text{ cm})$ equipped with built-in power, memory slot, USB port, Wi-Fi connectivity, motion detection, infrared vision, and loop recording capabilities. The motor bracket houses two bipolar stepper motors, which provide precise position and speed control by sequentially activating the stator coils. The component housing contains the power supply, control board, and communication modules, all compactly integrated. The motors drive the internal mechanism, facilitating the rolling motion of the spherical shell.

ELECTRONIC DESIGN

The Hibiscus Sense board is powered by the ESP32-DoWDQ6 chip (ESP32-WROOM-32), which integrates Wi-Fi, Bluetooth, and Bluetooth Low Energy (BLE) capabilities. It features a dual-core 32-bit LX6 CPU, 320 KB of RAM, and up to 16 MB of flash memory. Operating within a voltage range of 3.0–3.6 V DC and a temperature range of -40 to 85 °C, the board supports various interfaces, including GPIO, ADC, DAC, SPI, I²C, and UART. It is capable of handling functions such as audio streaming and low-power sensor networks. This board facilitates wireless communication between the spherical robot and a web browser or application-based graphical user interface (GUI) for real-time status monitoring and live video streaming. The A4988 stepper motor driver is used to control bipolar stepper motors in multiple stepping modes, ranging from full step to 1/16th microstepping. It supports input voltages of up to 35 V and can deliver output currents of up to ±2 A. The driver includes essential protection features such as overcurrent, short-circuit, under-voltage lockout, and over-temperature shutdown. Additionally, it incorporates a built-in translator, simplifying interface requirements with microcontrollers.



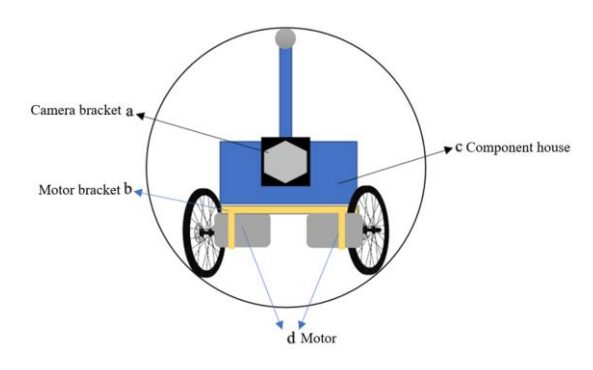


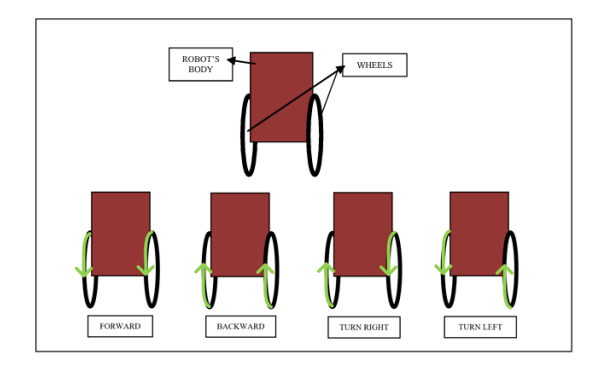
Fig 7. Robot Design

RESULTS AND DISCUSSION

The experiment involved evaluating the robot's directional movement using stepper motors configured with a setting pwm speed of 400 and an acceleration of 700, ensuring responsive and precise navigation. Figure 8 illustrates the basic motor movement patterns used for forward, backward, and turning motions.

The robot's adaptability, efficiency, mobility, and stability were tested across a variety of surfaces, including carpet, sand, grass, cement, and asphalt. These tests were conducted to determine the robot's optimal operating surface. Additionally, the onboard camera provided a real-time video feed and one-way connection to a smartphone, enabling live monitoring and video recording of the tests. This experimental assessment is essential for understanding the robot's interaction with different environmental conditions.

During testing, the spherical robot was assigned the task of navigating 2 meters toward a designated target across various types of terrain. This objective enabled the evaluation of the robot's performance and adaptability under different environmental conditions. As shown in Figure 9, the robot's ability to achieve the target was assessed through multiple trials. These tests focused on evaluating the robot's efficiency, maneuverability, and goal-reaching capability. The detailed performance metrics are presented in Table 1, while a summary of the test results is provided in Table 2.



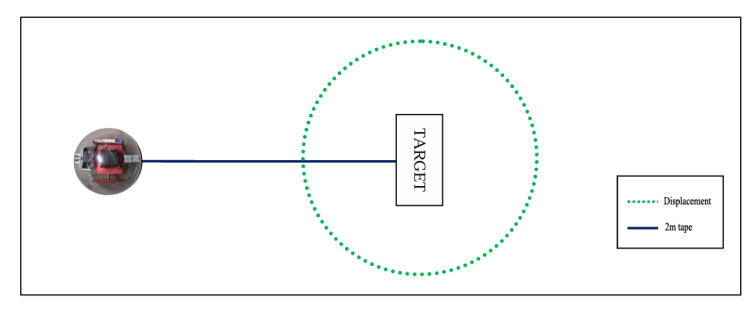


Fig 8. Illustration of the robot's Fig 9. Robot performance testing procedure movement



reaching the target

Terrain type No. of test Cement Grass Sand Tar road X

Table 1. The performance of the robot in Table 2. The displacement of the robot from the target

	Displacement from target (m)								
No. of test	Carpet	Cement	Grass	Sand	Tar road				
1	0.10	0.50	2.00	1.10	0.80				
2	0.20	0.80	2.00	1.20	1.10				
3	0.20 0.10		2.00	0.30	1.00				
4	0.50	0.20	2.00	0.40	0.40				
5	0.00	0.20	2.00	1.10	1.20				

A camera was strategically mounted on the robot during testing to record video footage and monitor the surrounding environment. The camera's performance was evaluated under both daytime and nighttime conditions to ensure optimal functionality. Figure 10 shows an image captured during daytime testing. In low-light environments, the camera automatically switches to infrared mode, enabling it to capture clear images even in the absence of visible light. This feature ensures reliable performance across varying lighting conditions. A key feature of the system is its ability to stream live video feeds to a smartphone, allowing real-time monitoring. This capability facilitates immediate response to any issues encountered during the robot's operation. Figure 11 illustrates the application's interface designed to control the movement of the spherical robot, accompanied by live video streaming from the integrated camera.





Fig 10. Robot's point of view during the day

Fig 11. Controlling App and view

CONCLUSION

The spherical robot demonstrated effective performance across a range of terrains, showing optimal functionality on carpet and cement surfaces, while encountering challenges on sand, grass, and tar roads. The integration of IMU sensor fusion significantly reduced drift and enhanced control accuracy and adaptability. Additionally, the onboard camera enabled real-time monitoring, with infrared functionality ensuring visibility under low-light conditions. This project underscored the critical role of robot-environment interaction and generated valuable data for further performance enhancement. Despite the challenges encountered, the design and testing processes have marked significant progress, contributing to the development of more intelligent and adaptable robotic systems.



ACKNOWLEDGMENT

The authors wish to thank Universiti Teknikal Malaysia Melaka for providing the equipment and resources necessary for the development of the spherical robot.

CONFLICT OF INTERESTS

Disclose any financial or personal relationships that could be perceived as influencing the research.

REFERENCES

- [1] S. Kuswadi, M. N. Tamara, B. T. Brahmantio, D. Sugiharto, and M. Nuh, "Disaster Robot Navigation using Behavior-based Systems," 2018 International Conference on Applied Science and Technology (iCAST), pp. 196–202, Oct. 2020, doi: 10.1109/icast51016.2020.9557734.
- [2] S. Kuswadi, S. I. Adji, R. Sigit, M. N. Tamara, and M. Nuh, Disaster swarm robot development: On going project. 2017, pp. 45–50. doi: 10.1109/iceltics.2017.8253258.
- [3] M. Bujňák et al., "Spherical Robots for Special Purposes: A review on current possibilities," Sensors, vol. 22, no. 4, p. 1413, Feb. 2022, doi: 10.3390/s22041413.
- [4] N. Q. Zhan, N. Y. Cai, and N. C. Yan, Design, analysis and experiments of an omni-directional spherical robot. 2011, pp. 4921–4926. doi: 10.1109/icra.2011.5980491.
- [5] W. Jia, Z. Huang, Y. Sun, H. Pu, and S. Ma, "Toward a novel deformable robot mechanism to transition between spherical rolling and quadruped walking," 2021 IEEE International Conference on Robotics and Biomimetics (ROBIO), pp. 1539–1544, Dec. 2017, doi: 10.1109/robio.2017.8324636.
- [6] N. Bun-Athuek and P. Laksanacharoen, "A new locomotion concept using shell transformation for a Reconfigurable Spherical Robot," Industrial Technology Lampang Rajabhat University Journal, vol. 13, no. 2, pp. 74–85, Jun. 2020, [Online]. Available: https://li01.tci-thaijo.org/index.php/Itech/issue/view/16988



CAMERA AUTO-CALIBRATION USING PARTICLE SWARM OPTIMIZATION

Lim Jing Wen¹, Amar Faiz Zainal Abidin^{1,*}, Rostam Affendi Hamzah¹, Nadzri Mohamood¹
Ali Abuasal, Mutaz Elsawi², Mohd Hezri Marzaki³

¹Faculty of Electronics & Computer Technology & Engineering, Universiti Teknikal Malaysia Melaka

²Faculty of Science and Technology, Université de Bourgogne

³School of Technology & Engineering Science, Wawasan Open University

*Correspondence: amarfaiz@utem.edu.my

ABSTRACT

Camera calibration is essential in ensuring the correct alignment of the captured images. There are numerous methods proposed to perform auto calibration of a camera proposed. This paper implements auto calibration camera method proposed by Mendonca and Cipolla. Particle Swarm Optimization is used to optimize the intrinsic parameters of the camera calibration. The result obtained is compared with the Levenberg–Marquart algorithm.

INTRODUCTION

Mendonca and Cipolla [1] proposed a method to perform auto calibration of a camera based on (1) where E is the essential matrix, F is the fundamental matrix and K is the intrinsic parameter matrix.

$$E \approx K^T F K \tag{1}$$

The intrinsic parameter matrix, K as stated in (2) consists of the following parameters: $\frac{f_u}{f_v}$ is the aspect ratio, s the skew, (u_0, v_0) represents the principal point.

$$\mathbf{K} = \begin{bmatrix} f_u & s & u_0 \\ 0 & f_v & v_0 \\ 0 & 0 & 1 \end{bmatrix} \tag{2}$$

The cost function, C in (3) is used to calculate the cost of the optimized K. Here, the objective is to minimize the cost.

$$C(\mathbf{K}, i = 1, ...n) = \sum_{i,j}^{n} \frac{\sigma_{ij}^{(1)} - \sigma_{ij}^{(2)}}{\sigma_{ij}^{(2)}}$$
(3)

where $\sigma_{ij}^{(1)}$ and $\sigma_{ij}^{(2)}$ are the non-zero singular value (SVD) of \boldsymbol{E} .



METHODS

A global optimization algorithm called Particle Swarm Optimization (PSO) is used to optimize the intrinsic parameters. PSO was introduced by J. Kennedy and R. Eberhert [2] and had been applied in many engineering problems [3]. PSO has Here a particle, s in PSO represented a candidate solution (parameters values) of the problem as shown in (4).

$$s = [f_u, s, u_0, f_v, v_0]$$
 (4)

Based on [2] and [3], Algorithm 1 shows the implementation PSO algorithm for camera auto calibration problem. The MATLAB source code can be obtained from [4].

Algorithm 1: Global Best PSO Algorithm for Camera Autocalibration Problem

```
01: initialize all particles by randomizing position based on (5)
02: while stopping condition not met
       for each particle, i do
03:
                calculate fitness for particle using (3)
04:
                if the particle fitness is better than previous pbest^k then
05:
                        set the particle fitness value as new pbest^k
06:
                        if the pbest^k is better than previous gbest
07:
                                set pbest^k as new abest
08:
09:
                        end if
                end if
10:
        end for
11:
        for each particle do
12:
                calculate particle velocity according to
13:
                v_{i,d}^{k+1} = \omega v_{i,d}^k + r_1 c_1 (v_{i,d}^k - \boldsymbol{pbest}^k) + r_2 c_2 (v_{i,d}^k - \boldsymbol{gbest})
update the particle position according to s_{i,d}^{k+1} = s_{i,d}^k + v_{i,d}^{k+1}
14:
        end for
15:
16: end while
```

The objective of PSO is to minimize the fitness function or cost which is stated in (3) where the best-found solution has the smallest cost.

The algorithm deals with the out-of-boundary condition by individually resetting the variable using the globe model. The globe model of out-of-boundary can be express mathematically as (5).

$$\mathbf{s}_{i,d}^{k,new} = \begin{cases} \mathbf{U}_d - (\mathbf{s}_{i,d}^k - \mathbf{L}_d) & \text{if } \mathbf{s}_{i,d}^k < \mathbf{L}_d \\ \mathbf{L}_d + (\mathbf{s}_{i,d}^k - \mathbf{U}_d) & \text{if } \mathbf{s}_{i,d}^k > \mathbf{K}_d \end{cases}$$
(5)

The stopping condition is triggered when the gbest solution obtained does not change after 50 iterations. Based on [2] and [3], Algorithm 1 shows the implementation PSO



algorithm for camera auto calibration problem. The MATLAB source code can be obtained from [4].

RESULTS AND DISCUSSION

Table 1 shows the parameters of PSO chosen for the study. The initial value of inertia weight, ω is 0.9 which slowly increases proportional to the number of iterations and ends at 0.4.

Table 1. The proposed intrinsic parameters matrix values.

Parameters	Value(s)
Number of computations	10
Number of agents	25
Inertia weight, ω	$0.9 \rightarrow 0.4$
Social coefficient, c_1	1.42
Cognitive coefficient, c_2	1.42

Table 2 shows the result obtained by PSO, the initial intrinsic parameters and Levenberg-Marquart algorithm (LMA) [5]. The best-found solution of LMA by [5] has a smaller cost compared to PSO. Having said that, the LMA algorithm is highly sensitive to the initial values of K assigned to it. On the other hand, PSO algorithm is less sensitive to the initial values of K assigned to it. This is due to the nature of PSO as stochastic-based optimization algorithm that thrive on unknown.

Table 2. The proposed intrinsic parameters matrix values.

		PSO		Initial			LMA [5]			
K (round	up	[801	0	256]	[870	0	279]	[800	0	256]
value)	-	0	800	256	0	812	261	0	800	256
1 0.12 0.0)		Lο	0	1]	L 0	0	1 J	Lο	0	1]
Cost		9.85	507×	10^{-4}	6.38	52 × 1	10^{-1}	1.60	51 × 1	0^{-13}

CONCLUSION

This paper presents the implementation of Mendonca and Cipolla model for camera auto calibration using PSO. The result is compared to the Lu Chipman method where the result indicates that PSO is inferior compared to Levenberg–Marquart algorithm.

ACKNOWLEDGMENT

This paper is based on one of the assignments of the subject in the Master of Science in Computer Vision program conducted by Université de Bourgogne.



REFERENCES

- P. R. S. Mendonca and R. Cipolla, "A simple technique for self-calibration," Proceedings. 1999 IEEE Computer Society Conference on Computer Vision and Pattern Recognition, pp. 500–505, Jan. 2003, doi: 10.1109/cvpr.1999.786984.
- [2] A. P. Engelbrecht, Fundamentals of Computational Swarm Intelligence. 2005. [Online]. Available: https://ci.nii.ac.jp/ncid/BA74316081
- [3] S. Khan, S. Anjum, U. A. Gulzari, F. Ishmanov, M. Palesi, and M. K. Afzal, "An optimized hybrid algorithm in term of energy and performance for mapping real time workloads on 2d based onchip networks," Applied Intelligence, vol. 48, no. 12, pp. 4792–4804, Jul. 2018, doi: 10.1007/s10489-018-1246-7.
- [4] A. F. Z. Abidin, "Source code for 3D Digitization: Camera Autocalibration Using Particle Swarm Optimization," http://tinyurl.com/afzabidin.
- [5] G. Lemaitre, "3D Digitization: Camera Autocalibration," http://tinyurl.com/84juvtr.



AUTOMATED PH-CONTROLLED WITH ALARM INTEGRATION FOR WATER TREATMENT SYSTEM

Muhammad Syukur Nurnekmah Azman¹, Nur Ezyanie Safie^{1,*}, Asri Din¹, Mohd Firdaus Tahirruddin²

¹Faculty of Electrical Technology and Engineering, Universiti Teknikal Malaysia Melaka

²IFFCO (Malaysia) Sdn. Bhd., Pasir Gudang, Johor, Malaysia

*Corresponding author: ezyanie@utem.edu.my

ABSTRACT

Effective pH control is critical in water treatment to maintain water quality and ensure regulatory compliance. This study presents the development of an IoT-based pH-controlled pre-treatment system implemented at an industrial water treatment plant in Malaysia. The system automates chemical dosing based on real-time pH monitoring and includes an alarm mechanism to detect deviations. It integrates high-accuracy pH sensors, a controller, and relay-activated alarm components. A 30-day field test was conducted, with data collected at four-hour intervals to assess pH stability and alarm responsiveness. Results showed that the system consistently maintained pH between 7.0 and 7.5, with minimal fluctuations and a standard deviation of ±0.17. The alarm system effectively flagged deviations, enabling prompt corrective actions. The implementation reduced manual labor, improved dosing precision, and enhanced operational safety. These findings demonstrate the system's potential for broader application in industrial water treatment environments.

INTRODUCTION

Maintaining chemical balance, particularly pH control, is vital in industrial water treatment processes to ensure system efficiency, protect infrastructure, and comply with environmental standards. pH imbalances can negatively impact coagulation, flocculation, and disinfection efficiency, while also causing pipe corrosion or scaling, ultimately leading to reduced water quality and higher maintenance costs. Conventional pH monitoring methods that rely on manual testing are prone to errors, delayed responses, and labor inefficiencies, which pose risks in fast-changing industrial environments [1]. These limitations highlight the need for more robust, automated solutions capable of continuous monitoring and real-time adjustments.

Recent advancements in industrial automation and IoT technologies have enabled the development of intelligent systems for water treatment. Automated dosing systems integrated with real-time sensors offer significant improvements in dosing precision, cost savings, and operational control [2]. Moreover, the inclusion of alarm-triggered responses enhances operational safety by ensuring immediate alerts when pH levels deviate from acceptable thresholds, thereby allowing for timely corrective actions. These smart systems support predictive maintenance strategies, lower the risk of



compliance violations, and contribute to more sustainable water management practices [3].

In this context, this study introduces and validates a pH-controlled pre-treatment system implemented at an industrial-scale water treatment plant in Malaysia. The system integrates high-precision pH sensors, programmable dosing controllers, and an automated alarm mechanism for real-time process regulation. Unlike earlier works limited to laboratory prototypes or simulations, this research emphasizes real-world deployment, offering practical insights into the system's performance under standard and high-load operational conditions. The findings provide a foundation for the scalable application of smart dosing systems across various sectors in industrial water treatment.

METHODS

This study employed a structured design methodology to develop an automated pH-controlled pre-treatment system for a water treatment plant. The research began with comprehensive requirements analysis, identifying operational parameters such as target pH range, chemical dosing needs, and alarm thresholds. Based on these specifications, high-accuracy EMEC pH controllers, combination pH electrodes, 3" MS-190 mini motor sirens, and industrial-grade indicators were selected for their reliability and compatibility with existing infrastructure.

As shown in Fig. 1, the system architecture was developed to integrate pH sensors with dosing pumps via a relay circuit, enabling real-time pH monitoring and automated chemical dosing. The alarm system was configured to activate when pH values deviated beyond preset thresholds, providing immediate operator alerts. Installation was carried out within IFFCO Malaysia's operational environment, and the system was tested over 30 consecutive days. Data was collected at 4-hour intervals using digital logs, capturing real-time pH values to assess stability and system responsiveness. Accuracy validation was performed using standard buffer solutions (pH 4.00, 7.00, and 10.00), with multiple trials to calculate average deviations.

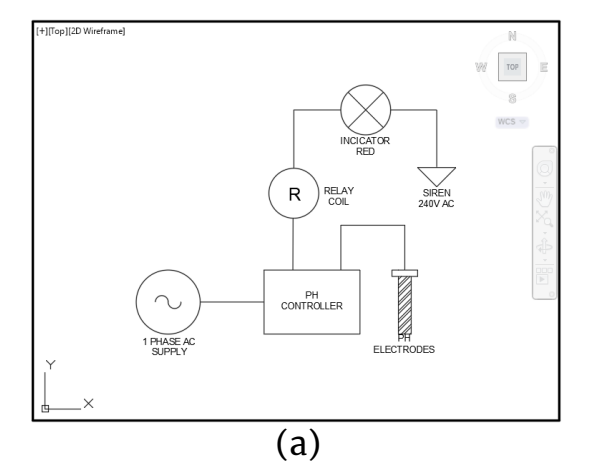




Fig 1. (a) Wiring diagram of the pH-controlled dosing system integrating a relay-triggered alarm and indicator mechanism; (b) Physical setup of the control panel installed at the treatment site, powered by a single-phase AC supply



RESULTS AND DISCUSSION

This section presents the findings from the development and deployment of a pH-controlled pre-treatment system designed to enhance the accuracy and control of chemical dosing in water treatment plant operations. The system incorporates high-precision pH sensors, and an integrated alarm mechanism designed to dynamically regulate chemical input in response to real-time pH fluctuations. To assess its performance, case studies were conducted within a full-scale industrial water treatment facility under both standard operational conditions and periods of elevated chemical load. These scenarios were selected to rigorously evaluate the system's adaptability and robustness, irrespective of external process variations. The evaluation spanned a one-month period, during which pH levels and chemical dosing adjustments were recorded at four-hour intervals. System efficacy was assessed through continuous monitoring, and the functionality of the alarm unit was validated based on its responsiveness to deviations beyond defined pH thresholds.

Table 1. Recorded pH levels at four-hour intervals over six days in June 2024, indicating consistent pH stability within the neutral range under normal operating conditions

Date (June2024)	Time	pH Level	Remarks
1	8:00 AM	7.2	normal
1	12:00 PM	7.4	normal
1	4:00 PM	7.3	normal
1	8:00 PM	7.1	normal
2	8:00 AM	7	normal
2	12:00 PM	7.2	normal
2	4:00 PM	7.3	normal
2	8:00 PM	7.5	normal
3	8:00 AM	7.1	normal
3	12:00 PM	7.3	normal
3	4:00 PM	7.4	normal
3	8:00 PM	7.2	normal
4	8:00 AM	7	normal
4	12:00 PM	7.1	normal
4	4:00 PM	7.3	normal
4	8:00 PM	7.2	normal
5	8:00 AM	7.0	normal
5	12:00 PM	7.2	normal
5	4:00 PM	7.0	normal
5	8:00 PM	7.5	normal
6	8:00 AM	7.3	normal
6	12:00 PM	7.4	normal
6	4:00 PM	7.1	normal



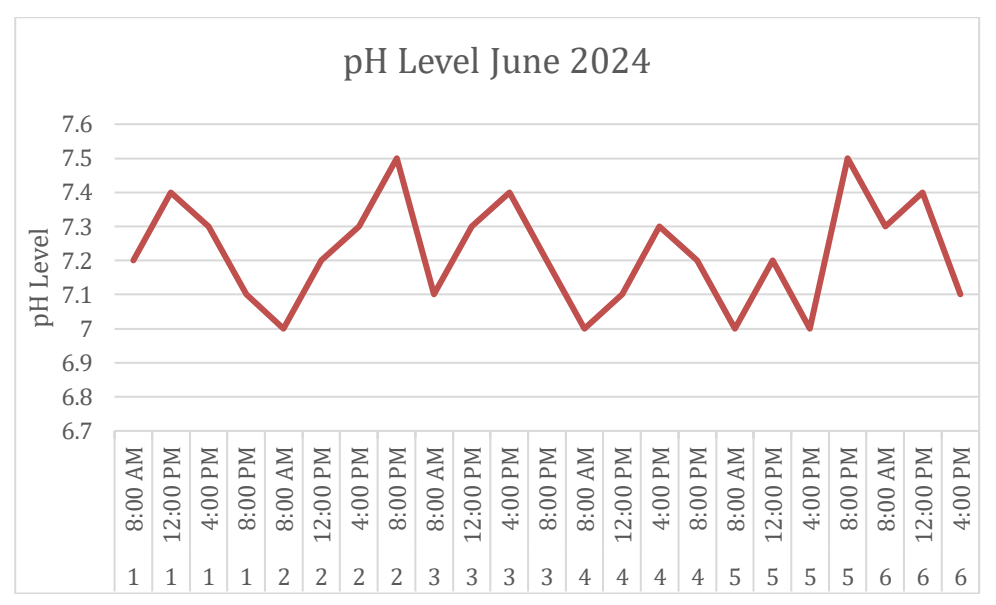


Fig 2. Line graph showing pH level variations recorded every four hours over six days in June 2024, demonstrating consistent maintenance within the neutral range.

The analysis of pH data collected over a 30-day monitoring period indicates the effectiveness of the developed pH-controlled pre-treatment system in maintaining chemical equilibrium within the water treatment process. As illustrated in Table 1 and Fig. 2, pH values ranged from 7.0 to 7.5, with an average value of approximately 7.2, demonstrating that the system consistently operated within the neutral range ideal for most treatment applications [4]. The minor diurnal fluctuations observed, with pH levels generally rising from morning to evening, are consistent with known operational dynamics in industrial settings, where thermal and flow variations influence chemical interactions. These variations remained within acceptable regulatory limits and did not necessitate significant dosing adjustments, suggesting system stability and robustness.

Notably, the ability of the system to autonomously regulate chemical dosing in response to real-time pH data underscores its precision and adaptability. The low standard deviation of pH readings (± 0.17) across time points reinforces the reliability of the control mechanism. This is consistent with findings from Taylor et al. (2019), who demonstrated that IoT-based feedback systems improve pH stability and reduce operational variance [5]. The system's integrated alarm function further enhanced its operational safety by issuing immediate alerts upon pH deviations, facilitating timely corrective actions and minimizing potential environmental or infrastructural risks.

The implementation also provided operational advantages by significantly reducing manual interventions. Previously, plant personnel depended on portable pH testers, which are time-consuming and susceptible to user error. By automating this process, the system not only improved data accuracy but also reduced labor demands and exposure to hazardous chemicals. This aligns with recommendations in contemporary industrial best practices that advocate for automation to enhance both safety and efficiency in chemical dosing systems [6].



While the system performed effectively under both normal and high-load conditions, certain limitations were identified. The monitoring was restricted to pH levels, excluding other influencing variables such as temperature, flow rate, or total dissolved solids that may impact treatment efficacy. Furthermore, the study employed basic statistical analysis, and future work should incorporate predictive algorithms using machine learning to anticipate chemical demand shifts more proactively [7].

In summary, the study affirms that the integration of a real-time pH monitoring and alarm system significantly enhances the control and safety of chemical dosing in water treatment. These findings support broader implementation in industrial applications, with the potential for optimization through integration with multi-parameter sensing and AI-driven control frameworks.

Conclusion

Integrating automated pH control and alarm notification into water treatment operations has proven to be a reliable and efficient strategy for optimizing chemical dosing. The system demonstrated the ability to maintain stable pH levels within narrow tolerances, even under varying chemical load conditions, thereby ensuring consistent water quality and regulatory compliance. By reducing the need for manual intervention, the approach enhances operational safety and efficiency, making it highly suitable for industrial–scale applications. The methodology also facilitates systematic performance assessment, offering a replicable model for similar water treatment environments. As environmental regulations tighten and demand for sustainable practices increases, such automated systems offer a scalable solution for modernizing water treatment infrastructure.

ACKNOWLEDGMENT

The authors would like to express their sincere appreciation to Universiti Teknikal Malaysia Melaka (UTeM) and IFFCO (Malaysia) Sdn. Bhd. for their valuable collaboration in the Work-Based Learning (WBL) program under the Bachelor of Technology curriculum. This project was carried out in response to a real industrial challenge identified during the WBL placement.

CONFLICT OF INTERESTS

The author declares no conflict of interest.

REFERENCES

- [1] P. Jayaraman, K. K. Nagarajan, P. Partheeban, and V. Krishnamurthy, "Critical review on water quality analysis using IoT and machine learning models," International Journal of Information Management Data Insights, vol. 4, no. 1, p. 100210, Jan. 2024, doi: 10.1016/j.jjimei.2023.100210.
- [2] H. M. Forhad et al., "IoT based Real-Time Water Quality Monitoring system in Water Treatment Plants," Heliyon, vol. 10, no. 23, p. e40746, Nov. 2024, doi: 10.1016/j.heliyon.2024.e40746.
- [3] S. W. Goh et al., "Recent advancements in smart materials for the removal of organic, inorganic and microbial pollutants in water treatment: A review," Journal of Water Process Engineering, vol. 70, p. 106993, Jan. 2025, doi: 10.1016/j.jwpe.2025.106993.



- [4] Walchem, Iwaki America Inc., "The importance of pH control in water treatment processes," Walchem, May 19, 2025. https://www.walchem.com/the-importance-of-ph-control-in-water-treatment-processes/
- [5] G. A. Taylor et al., "PH Measurement IoT system for precision agriculture applications," IEEE Latin America Transactions, vol. 17, no. 05, pp. 823–832, May 2019, doi: 10.1109/tla.2019.8891951.
- [6] T. Hariono and M. C. Putra, "Data acquisition for monitoring IoT-Based hydroponic Automation system using ESP8266," NEWTON Networking and Information Technology, vol. 1, no. 1, pp. 1–7, Jun. 2021, doi: 10.32764/newton.v1i1.1534.
- [7] P. Megantoro et al., "Instrumentation system for data acquisition and monitoring of hydroponic farming using ESP32 via Google Firebase," Indonesian Journal of Electrical Engineering and Computer Science, vol. 27, no. 1, p. 52, Jun. 2022, doi: 10.11591/ijeecs.v27.i1.pp52-61.



TEMPERATURE IMPROVEMENT ACCURACY USING RESISTANCE TEMPERATURE DETECTOR (RTD) FOR PRODUCT QUALITY

Muhammad Yazid Zahid¹, Nur Ezyanie Safie^{1,*}, Sulaiman Sabikan¹
Mohd Firdaus Tahirruddin²

¹Faculty of Electrical Technology and Engineering, Universiti Teknikal Malaysia Melaka

²IFFCO (Malaysia) Sdn. Bhd., Pasir Gudang, Johor, Malaysia.

*Corresponding author: ezyanie@utem.edu.my

ABSTRACT

Accurate temperature control is vital in manufacturing to maintain product quality and meet regulatory standards. This study investigates the use of PT100 Resistance Temperature Detectors (RTDs) at IFFCO (Malaysia) to enhance monitoring precision and process stability. A 3-wire RTD configuration was integrated with Yokogawa Distributed Control Systems, supported by calibration, feasibility, and cost-benefit analyses. Results showed that RTDs outperformed conventional sensors in accuracy (±0.1°C), responsiveness, and reliability across a wide temperature range (-200°C to 600°C). Despite higher initial costs, the system delivered long-term savings via improved energy efficiency and reduced maintenance. RTD integration proved both technically and economically feasible, offering a robust solution for industrial temperature monitoring and improved operational outcomes.

INTRODUCTION

Temperature control plays a critical role in modern industrial manufacturing processes, influencing product consistency, energy efficiency, and regulatory compliance. Precise temperature measurement is essential for quality assurance in sectors such as food processing, chemical manufacturing, and pharmaceuticals. Traditional thermometric devices, such as thermocouples, often suffer from limitations including nonlinear output, signal drift, and limited environmental adaptability. To address these shortcomings, Resistance Temperature Detectors (RTDs), particularly the PT100 type, have emerged as a preferred choice due to their superior accuracy, linearity, and long-term stability across a broad operational range [1].

RTDs operate on the principle that the electrical resistance of a metal increases with temperature, with platinum being the most widely used sensing element due to its predictable resistance–temperature relationship and corrosion resistance. The PT100 variant, characterized by a resistance of 100 ohms at 0°C, is especially noted for its stability and repeatability in harsh industrial environments [2]. Integration of these sensors into modern control architectures, such as Distributed Control Systems (DCS),



allows for real-time feedback and fine-tuned process regulation. Three-wire RTD configurations, in particular, offer a balanced solution by compensating for lead resistance without the added complexity and cost of four-wire setups [3].

This study explores the implementation of PT100 RTDs within IFFCO (Malaysia)'s industrial process lines to assess improvements in temperature monitoring precision, response time, and system integration. A comprehensive approach combining technical calibration, feasibility assessment, and user-centered evaluation was adopted. Previous investigations have demonstrated the potential of RTDs in both rigid and flexible applications, such as thick-film printed RTDs on specialized substrates for real-time monitoring of furnaces and complex geometries [4]. The present research builds upon these advancements by demonstrating the practical feasibility, operational reliability, and economic advantages of RTD-based systems in large-scale industrial deployments.

METHODS

The temperature monitoring enhancement was achieved through the design, calibration, and integration of a PT100 Resistance Temperature Detector (RTD) using a three-wire configuration. The physical dimensions and structure of the RTD sensor, including stem length, fitting depth, and sensor radius (L1–L4, R), are illustrated in Fig. 1 (a), ensuring compatibility with industrial tank installations. Calibration and system validation were conducted using a controlled setup comprising a HART Communicator 475, a digital multimeter, and a precision temperature bath, as shown in Fig. 1 (b). This setup facilitated accurate configuration and cross-validation of sensor readings under stable thermal conditions.

The signal acquisition strategy involved two configurations: direct wiring of the RTD sensor to the control system and an alternative route via a 4–20 mA transmitter, as outlined in Fig. 1 (c). The transmitter approach enabled signal standardization for long-distance transmission and noise resilience, enhancing compatibility with distributed control environments. Electrical integration of the RTD into the control network was carried out using a standardized three-wire wiring scheme (Fig. 1(d)). This configuration compensates for lead resistance, thereby preserving measurement fidelity across extended cable lengths. The wiring connections were terminated at a terminal head and interfaced with the Yokogawa Distributed Control System (DCS) to enable real-time data logging, PID-controlled feedback loops, and alarm systems for process optimization.



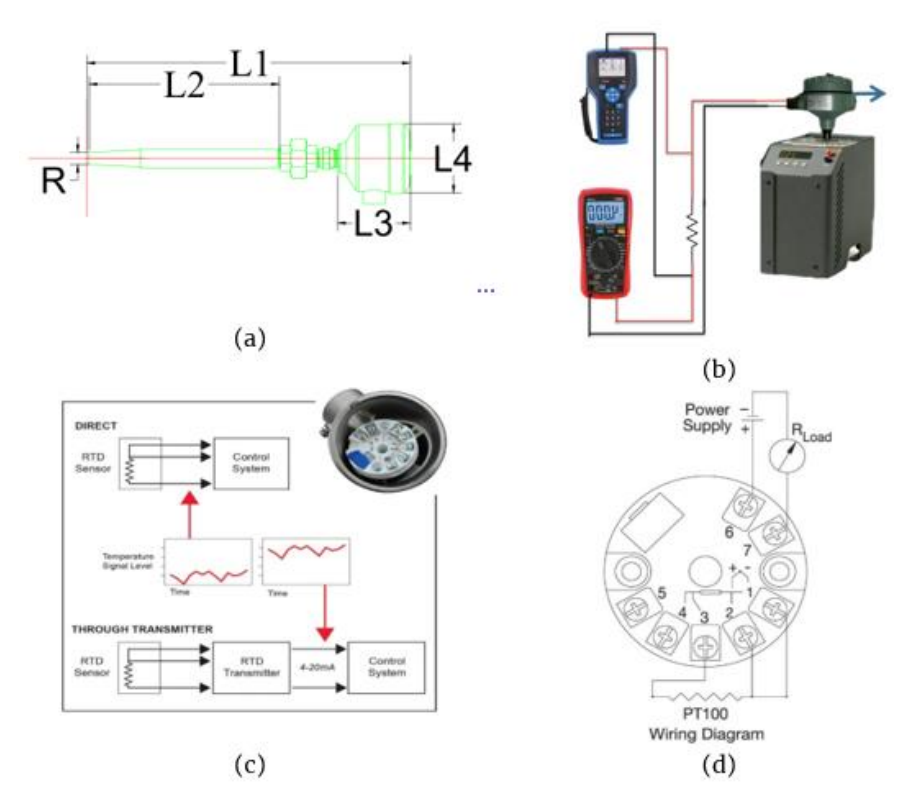


Fig 1. (a) Dimensional schematic of the RTD PT100 sensor, indicating critical measurement lengths (L1–L4) and sensor radius (R). (b) Experimental setup for RTD calibration using HART Communicator 475, multimeter, and temperature bath system. (c) Signal transmission pathways from RTD sensors: direct connection to control systems versus via 4–20 mA transmitter integration. (d) Terminal wiring diagram for PT100 RTD sensor illustrating three-wire configuration and connection to power supply and load.

RESULTS AND DISCUSSION

The evaluation of the RTD PT100 three-wire sensor system was conducted through systematic calibration, integration testing, and operational monitoring within an industrial tank environment. Calibration results from four RTD units (TIC 20103–TIC 20106) were analyzed to verify measurement stability and conformity with thermal standards. Each sensor was subjected to a series of temperature setpoints using a controlled bath and validated against digital reference instruments. The calibration reports confirmed consistent response behavior across the operational range (0–300°C), affirming the efficacy of the three-wire configuration in minimizing lead resistance and ensuring accurate signal integrity. This is consistent with findings by Kartika et al. (2024), who noted the high precision and low error rates of PT100 sensors when calibrated through regression–based approaches for industrial systems [5].

Following deployment, temperature monitoring data demonstrated steady thermal behavior across upper, central, and lower tank regions. Sensors TIC 20103 (top), TIC 20104 and TIC 20105 (center), and TIC 20106 (bottom) exhibited minimal deviation, confirming uniform thermal distribution and indicating effective sensor positioning and process control. The plotted sensor data (Fig. 2) illustrate stable hourly readings



without abrupt fluctuations, reflecting controlled heating dynamics and robust system integration.

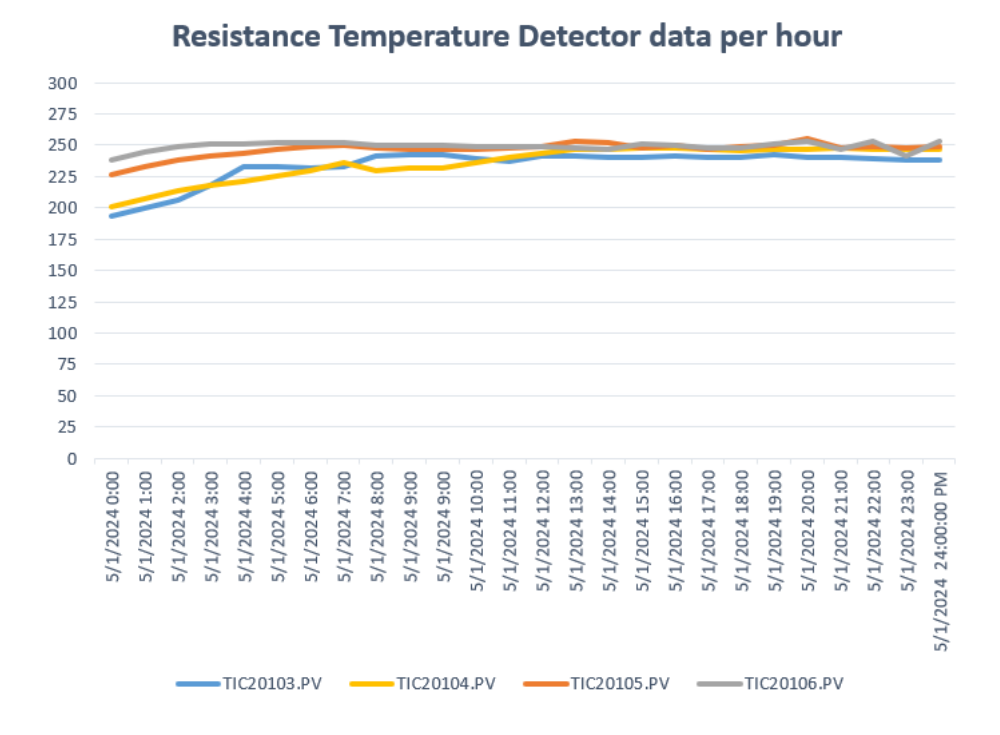


Fig 2. Hourly temperature readings from four RTD PT100 sensors (TIC20103–TIC20106) recorded on May 1, 2024. The data shows stable and consistent thermal behavior across different tank positions (top, center, and bottom), with temperatures generally ranging between 225°C and 260°C, indicating effective thermal regulation and process control.

To assess the system's usability, a structured user feedback survey was distributed to operators and instrumentation staff. Survey metrics captured user perceptions on five criteria: system control, operational simplicity, design aesthetics, wiring clarity, and the need for modification. The summarized responses shown in Fig. 3, reveal high satisfaction with interface usability (80%) and connection clarity (70%), with moderate scores for aesthetics (60%) and operational ease (50%). A 40% response rate on modification needs indicates areas for potential ergonomic or functional improvement.



Bar Chart: Criteria Ratings for the Yokogawa System and RTD PT 100

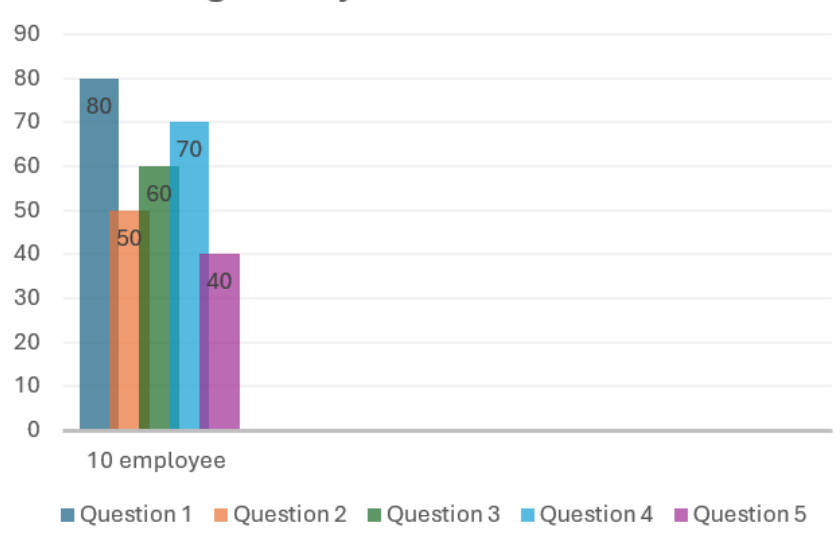


Fig 3. User evaluation of the RTD PT100 system and Yokogawa interface based on five performance criteria

These results validate the feasibility of RTD PT100 integration in complex process environments. The system not only achieved high accuracy and process stability but also received favorable user feedback, highlighting its potential for scalable industrial deployment. Nonetheless, opportunities exist to enhance operational simplicity and visual ergonomics for improved long-term user experience. These observations echo findings by Li (2024), who emphasized the importance of calibration and environmental compensation in maintaining the long-term reliability of RTD-based systems in industrial environments [6].

CONCLUSION

This study successfully demonstrated the technical, operational, and economic advantages of implementing RTD PT100 sensors for precision temperature monitoring within IFFCO (Malaysia) Sdn Bhd. The deployment of 3-wire RTD PT100 technology, supported by a thorough technical assessment and cost-benefit analysis, significantly improved measurement accuracy, response stability, and control system integration. Compared to conventional temperature sensors, RTDs provided superior repeatability and reliability, enabling more consistent process control and reducing the incidence of thermal deviation.

The integration of RTDs into the Yokogawa Distributed Control System (DCS), combined with real-time data acquisition and PID control algorithms, facilitated enhanced energy efficiency, reduced maintenance demands, and improved overall product quality. Temperature readings remained consistently within the operational range $(0-300^{\circ}\text{C})$, confirming the sensors' suitability for critical process applications.



These improvements underscore the value of RTD PT100 systems as scalable and adaptable solutions for diverse industrial settings.

Moreover, this research contributes to the broader industrial discourse by validating RTD PT100 technology as a viable and cost-effective alternative for manufacturers seeking to upgrade legacy temperature monitoring infrastructure. The findings highlight not only short-term process optimization but also long-term sustainability through reduced waste, improved operational reliability, and alignment with quality assurance standards. In sum, RTD PT100 sensors emerge from this study not merely as instrumentation components, but as strategic assets for advancing industrial efficiency and thermal process integrity.

ACKNOWLEDGMENT

The authors would like to express their sincere appreciation to Universiti Teknikal Malaysia Melaka (UTeM) and IFFCO (Malaysia) Sdn. Bhd. for their valuable collaboration in the Work-Based Learning (WBL) program under the Bachelor of Technology curriculum. This project was carried out in response to a real industrial challenge identified during the WBL placement.

CONFLICT OF INTERESTS

The author declares no conflict of interest.

REFERENCES

- [1] C. Dames, "Resistance temperature detectors," in Springer eBooks, 2008, pp. 1782–1790. doi: 10.1007/978-0-387-48998-8 1354.
- [2] Z. Hai, Z. Su, K. Zhu, Y. Pan, and S. Luo, "Printed Thick Film Resistance Temperature Detector for Real-Time tube Furnace temperature monitoring," Sensors, vol. 24, no. 10, p. 2999, May 2024, doi: 10.3390/s24102999.
- [3] N. P. S. M. Saad, N. N. A. H. A. Halim, N. H. Zulkefle, N. N. Ahmad, and N. S. S. Sivaraju, "Precision Temperature Measurement and Error Analysis for Three-Wire PT100 Resistance Temperature Detector (RTD) using LTSpice," Journal of Advanced Research in Fluid Mechanics and Thermal Sciences, vol. 118, no. 2, pp. 148–159, Jul. 2024, doi: 10.37934/arfmts.118.2.148159.
- [4] V. S. Turkani et al., "Nickel based printed Resistance temperature detector on flexible polyimide substrate," IEEE Sensors, pp. 1–4, Oct. 2018, doi: 10.1109/icsens.2018.8589549.
- [5] K. Kartika, A. Asran, M. P. Hasibuan, and M. Misriana, "Implementation of linear regression method for calibration and temperature measurement on PT100 temperature sensor," Jurnal Elektronika Dan Otomasi Industri, vol. 11, no. 2, pp. 503–511, Jul. 2024, doi: 10.33795/elkolind.v11i2.5206.
- [6] H. Li, "Pt100 temperature measurement sensors design and transducer simulation," Journal of Physics Conference Series, vol. 2897, no. 1, p. 012011, Nov. 2024, doi: 10.1088/1742-6596/2897/1/012011.



DEVELOPMENT OF A TEMPERATURE-CONTROLLED MOTOR STABILIZATION SOLUTION FOR HIGH-SPEED TESTING MACHINES

Ahmad Harith Mohamad Ghazali¹, Nur Ezyanie Safie^{1,*}, Ahmad Zubir Jamil¹,

Jefri Meser², Lee Ming Huei²

¹Faculty of Electrical Technology and Engineering, Universiti Teknikal Malaysia Melaka

²Cohu Malaysia Sdn. Bhd., Kawasan Perindustrian Ayer Keroh, Melaka, Malaysia

*Corresponding author: ezyanie@utem.edu.my

ABSTRACT

Motor overheating and misalignment pose significant challenges in highspeed semiconductor testing, often leading to structural deformation, reduced accuracy, and potential system failure. To address these issues in Neon Inspection Handler, a temperature-controlled stabilization system was developed, integrating thermal sensors, automated ventilation, and adaptive Z-axis controls. At speeds of 60,000 units per hour, motor temperatures previously peaked at 63°C, triggering mechanical shifts exceeding 100 mm. With the implemented solution, temperatures were reduced to 46°C, and PUH displacement was minimized by 70%, restoring alignment and operational reliability. The outcome underscores the importance of real-time thermal management in preserving precision and equipment lifespan high-throughput extending in industrial environments.

INTRODUCTION

High-speed testing machines are integral to semiconductor, medical, and electronics manufacturing, where consistent mechanical precision and operational reliability are critical. A major operational limitation in these systems stems from motor-induced thermal fluctuations, which can lead to structural deformation, positional inaccuracies, and ultimately, reduced throughput quality. As the demand for high-speed performance increases, so does the motor's thermal load, resulting in expanded components and compromised mechanical tolerances.

For example, Li et al. (2024) showed that high-strength silicon steels used in motor rotors experience magnetic property degradation under thermal stress, directly impacting torque and rotational efficiency [1]. Similarly, Chu et al. (2020) emphasized the importance of incorporating temperature-dependent material properties in the design of permanent magnet motors to ensure operational reliability at high speeds [2]. Thermal expansion in core components has been shown to induce radial misalignments, as analyzed in finite element simulations, revealing that uncontrolled heat buildup can cause over 250 °C temperature rises in critical areas [3].



Despite technological progress in sensor integration and control loops, challenges persist in ensuring real-time thermal stability during machine acceleration. Zeng et al. (2023) highlighted how structural reliability deteriorates with temperature when interference fits are poorly optimized, reinforcing the need for dynamic control systems [4]. Additionally, recent work by Yan et al. (2024) has stressed the role of magnetic hysteresis and iron losses at elevated temperatures, where performance simulations diverged from real-world behavior without temperature corrections [5].

Given this background, the present study aims to develop and evaluate a temperature-controlled stabilization system capable of mitigating thermal drift in high-speed testing machines. This research is rooted in an industrial problem faced by Cohu Malaysia, a leading provider of automated test handling solutions. Specifically, it addresses the thermal instability observed in the Neon Inspection Handler, a high-speed semiconductor test platform. Operators reported that at elevated speeds, the torque motor's rising temperature caused misalignment between the Pick-Up Head and pusher mechanism, increasing the risk of collision and reducing inspection accuracy. This real-world challenge underscores the need for a robust, temperature-aware stabilization strategy tailored for high-throughput environments.

METHODS

This study employed a structured experimental approach to evaluate the thermal impact on mechanical precision in a high-speed semiconductor handler. Testing was conducted in three phases: baseline assessment, control system implementation, and performance validation. The primary focus was to quantify motor temperature rise and its correlation with Z-axis displacement under elevated speeds. Thermal data were collected using PT1000 resistance temperature detectors positioned at key locations of the Neon Inspection Handler, including the torque motor, IND-Z bracket, INS-Z housing, and barrel-foot interface, as depicted in Fig 1 (a)-(c). Mechanical displacement was measured using high-precision micrometer dial gauges and laser displacement sensors with $\pm 1~\mu m$ accuracy. Sensor calibration followed traceable standards, and data logging was continuous over a 150-minute cycle at machine speeds ranging from 30,000 to 60,000 units per hour.

To regulate temperature, a control system was developed where ventilation was triggered automatically when motor temperature exceeded 63°C. Cooling was deactivated once conditions stabilized near 45°C. Simultaneously, vertical alignment was preserved using an Independent-Z actuator with encoder-based feedback to maintain pusher-PUH clearance during thermal expansion. Displacement and temperature data were analyzed using descriptive statistics and visualized through time-series graphs. Repeatability was verified through multiple trials, ensuring consistency and reproducibility of the results. This methodology enabled real-time assessment of thermal effects and validated the effectiveness of the proposed control system.



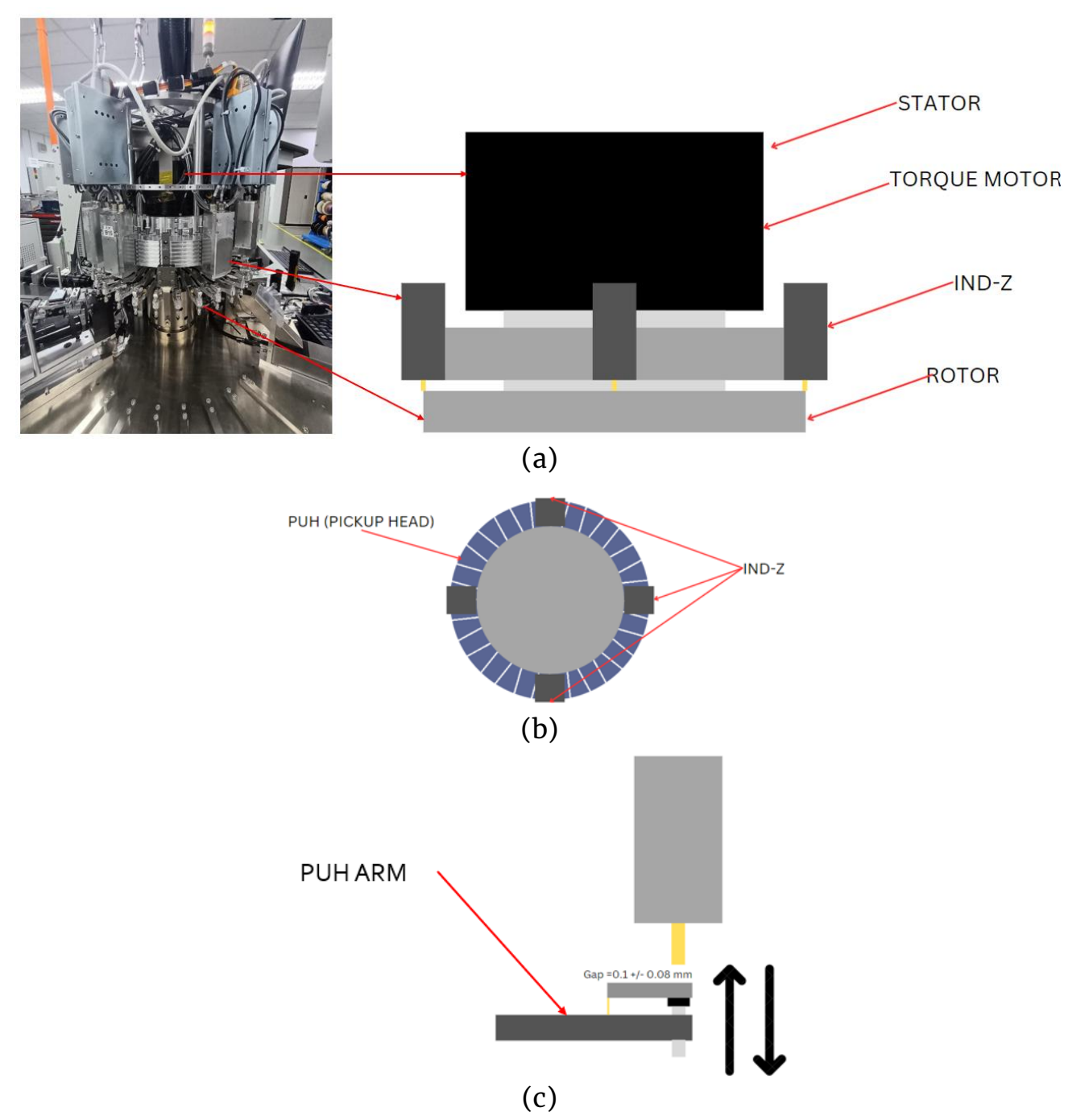


Fig 1. Structural Configuration of the Neon Inspection Handler (a) Assembly layout showing the torque motor, stator, rotor, and Independent–Z (IND–Z) components, (b) Top–down schematic of the PUH (Pick–Up Head) arrangement around the rotary structure, (c) Cross–sectional view of the PUH arm and IND–Z highlighting the vertical clearance critical for thermal displacement analysis.

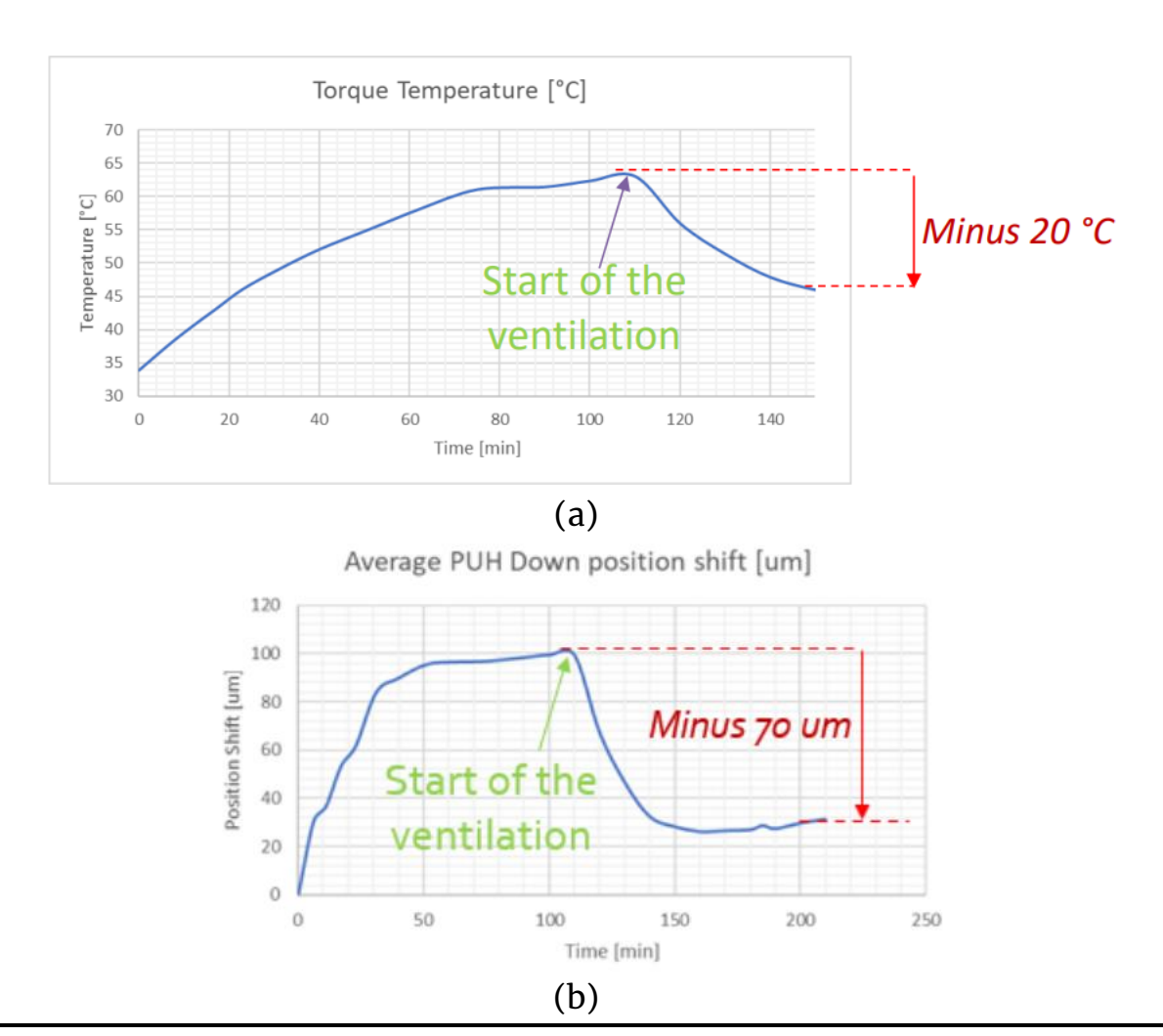
RESULTS AND DISCUSSION

This study examined the thermal impact on mechanical alignment using precision instrumentation, including thermal sensors, micrometer dial gauges, and laser metrology systems. Testing was performed under uncooled and cooled conditions to evaluate the system's stability and positional accuracy.



When the machine's operating speed increased from 30,000 to 60,000 units per hour (UPH), the torque motor temperature rose to 63°C, triggering thermal expansion. This temperature elevation led to significant mechanical displacement in key structural components. For instance, the PUH experienced a downward shift of approximately 100 mm and an upward shift of 15 mm with variability across heads. The IND–Z bracket also showed a vertical displacement ranging between 100 and 110 mm. These shifts reduced the clearance between the pusher and PUH, introducing a substantial risk of component collision. The correlation between thermal rise and mechanical instability has been well documented in high–speed motor research, where increased operating temperatures alter magnetic and structural performance, reducing mechanical tolerance and efficiency [5].

To address these challenges, a temperature-controlled ventilation mechanism was introduced. This system was activated at the 120-minute mark, effectively reducing motor temperature by 20°C. As shown in Fig. 2 (a), the temperature dropped from 63 to 43°C, and this reduction was directly reflected in mechanical behavior. PUH downward displacement improved by 70 mm (Fig. 2 (b)), and the upward shift decreased by 16 mm (Fig. 2 (c)). These results confirm that temperature management significantly mitigates thermally induced drift and positional deviation. Similar findings were observed in studies on permanent magnet motors under thermal stress, where optimized thermal control improved torque stability and reduced structural stress [6].





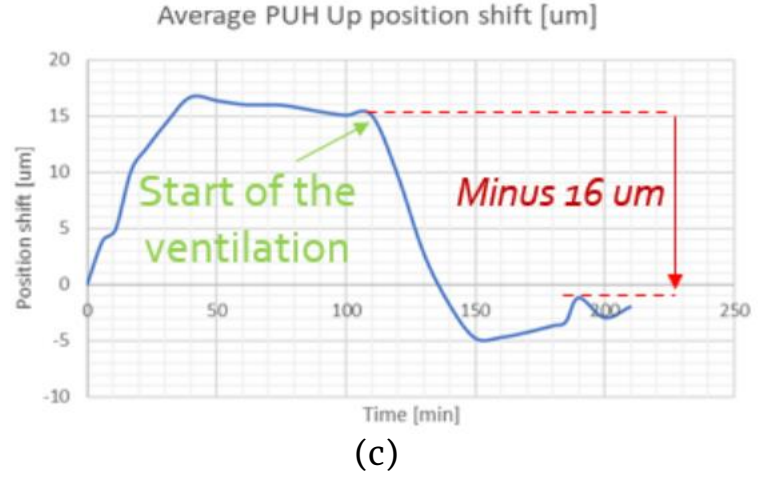


Fig 2. Effect of Ventilation Activation on System Parameters (a) Torque motor temperature reduced by 20°C after ventilation, (b) PUH downward position shift decreased by 70 μ m, (c) PUH upward position shift decreased by 16 μ m, indicating enhanced thermal stability and mechanical precision.

The combined data reinforce the conclusion that thermal regulation through active ventilation and real-time sensor integration is effective in controlling dimensional variance and improving machine stability. This hybrid approach to thermal management ensures consistent operational accuracy and is adaptable for broader industrial applications involving high-speed automated systems.

Comparative Evaluation

Upon implementing the hybrid solution, the motor temperature stabilized at an average of 46°C. Correspondingly, mechanical displacement values showed a marked reduction. The PUH downshift was limited to 30 mm, while the upward shift was controlled at -1 mm, ensuring consistent gap maintenance. These results indicated substantial improvement in positional accuracy and thermal control. A comparative analysis between pre- and post-implementation metrics underscores the effectiveness of the proposed solution. Before intervention, the PUH exhibited a downshift of 100 mm, and the torque motor temperature rose to 63°C. Post-intervention data revealed a significant improvement, with PUH displacement reduced and operating temperature maintained below 45°C. The summary of these values is presented in Table 1.



Table 1. Comparative Evaluation of PUH Displacement, Z-Axis Shift, and Temperature Before and After Thermal Control Implementation at Various Machine Speeds

Speed	PUH (Pick Up Head) Up Pos	PUH (Pick Up Head) Down Pos	PUH Arm Shift	IND-Z bracket	Temperature	Time (min)
BEFORE						
30k UPH	11	60	17	60	45°C	20
60k UPH	15	100	42	100- 110	63°C	110
AFTER						
60k UPH	15	100	47	100- 110	63°C	100
60k UPH	-1	30	10	30	33°C	150

CONCLUSION

The implementation of a temperature–regulated stabilization system for high–speed motor applications demonstrated significant improvements in thermal control, positional accuracy, and mechanical stability. Before the intervention, the motor temperature peaked at 63°C, resulting in substantial mechanical displacements. These included a downward shift of 100 mm in the Pick–Up Head and a displacement of up to 110 mm at the IND–Z bracket. Such temperature–induced deformations compromised machine alignment and increased the risk of component interference. After integrating a hybrid system that combined sensor–based thermal monitoring with automated ventilation control, the operating temperature was reduced to an average of 46°C. This thermal reduction was accompanied by a marked improvement in mechanical positioning. The downward displacement of the Pick–Up Head decreased to 30 mm, while the upward shift stabilized within minus 1 mm, reflecting enhanced dimensional consistency.

The data confirmed that temperature fluctuations had a direct impact on mechanical behavior. Following system implementation, the Pick-Up Head arm shift was reduced from 42 mm to 10 mm. Similarly, the IND-Z bracket displacement improved from over 100 mm to 30 mm, indicating a 70 % enhancement in structural precision. These improvements were sustained at an operational speed of 60 thousand units per hour, demonstrating that thermal compensation measures could be applied without compromising productivity. The ability to maintain high accuracy under elevated



throughput conditions supports the effectiveness of this integrated approach in precision-focused environments.

This study contributes a validated engineering solution for addressing thermal-mechanical instability in motor-driven systems. By integrating real-time temperature feedback with automated cooling and positional adjustment, the system provided consistent performance, reduced thermal stress, and improved reliability. These outcomes reinforce the feasibility of scalable and adaptable thermal control architectures for industrial applications. Furthermore, the research lays a foundation for future exploration into predictive control algorithms, advanced cooling technologies, and real-time stabilization strategies that can further enhance the efficiency and longevity of high-speed motor systems.

ACKNOWLEDGMENT

The authors would like to express their sincere appreciation to Universiti Teknikal Malaysia Melaka (UTeM) and Cohu Malaysia Sdn. Bhd. for their valuable collaboration in the Work-Based Learning (WBL) program under the Bachelor of Technology curriculum. This project was carried out in response to a real industrial challenge identified during the WBL placement.

CONFLICT OF INTERESTS

The author declares no conflict of interest.

REFERENCES

- [1] Y. Li, C. Yan, A. Wang, J. Li, L. Zeng, and R. Pei, "Study on the performance of a High-Speed Motor, considering the effect of temperature on the properties of High-Strength Non-Oriented silicon Steel," Materials, vol. 17, no. 9, p. 1936, Apr. 2024, doi: 10.3390/ma17091936.
- [2] S. Chu, D. Liang, S. Jia, and Y. Liang, "Research and analysis on design characteristics of high temperature and high-speed permanent magnet motor," 2022 International Conference on Electrical Machines (ICEM), Aug. 2020, doi: 10.1109/icem49940.2020.9270887.
- [3] W. Hao, L. Deliang, J. Shaofeng, C. Shuaijun, and L. Yongtao, "Analysis of the temperature field of a High-Speed Permanent Magnet Motor," in Lecture notes in electrical engineering, 2021, pp. 397–407. doi: 10.1007/978-981-33-6609-1_35.
- [4] Y. Zeng et al., "Influence of interference fit and temperature on High-Speed Permanent Magnet Motor," Applied Sciences, vol. 13, no. 20, p. 11331, Oct. 2023, doi: 10.3390/app132011331.
- Y. Gu, X. Wang, P. Gao, and X. Li, "Mechanical analysis with thermal effects for High-Speed Permanent-Magnet synchronous machines," IEEE Transactions on Industry Applications, vol. 57, no. 5, pp. 4646–4656, Jun. 2021, doi: 10.1109/tia.2021.3087120.
- [6] A. Tameemi, "Influence of high temperature on electromagnetic and mechanical performances of High-Speed Permanent Magnet machines," 2021 IEEE International Power and Renewable Energy Conference (IPRECON), pp. 1–5, Dec. 2022, doi: 10.1109/iprecon55716.2022.10059503



SOLAR CHARGING MONITORING SYSTEM USING ARDUINO UNO FOR LIGHTING APPLICATION

Mohamad Fazli bin Abdul Rani¹, Suziana Ahmad^{1,*}, Nurul Syuhada binti Mohd Shari¹ ¹Faculty of Electrical Technology and Engineering, Universiti Teknikal Malaysia Melaka *Corresponding author: suziana@utem.edu.my

ABSTRACT

This paper presents a solar charging monitoring system using Arduino Uno, developed for efficient lighting control in off-grid applications. The system comprises a solar panel, charge controller, 12V battery, LDR sensor, and LED light. The Arduino Uno automates the system by detecting ambient light through the LDR sensor and activating the LED light using a relay module. Voltage and current values are monitored via sensors and displayed on an LCD screen for real-time evaluation. The system was tested to assess power generation and consumption patterns throughout the day. Results indicate that the solar panel generates higher voltage later in the day, while the full system peaks earlier and gradually decline. A noticeable power drop between input and output highlights energy losses due to system inefficiencies.

INTRODUCTION

Electricity plays a vital role in modern life, with society heavily dependent on it for various applications [1]. Solar energy, derived from the sun's electromagnetic emissions, is the most abundant and environmentally friendly energy source. Its adoption has increased globally due to easy installation and low maintenance. Using photovoltaic (PV) technology, solar energy is converted into electricity, powering homes, appliances, climate systems, and transportation. However, supply remains insufficient, especially in developing countries where high electricity costs limit access [2]. A major challenge in implementing solar charge controller systems is limited clean energy access in remote areas. Conventional sources still pose serious environmental threats [4], [5]. Despite solar's sustainability and low emissions, barriers such as high initial cost, maintenance, technical expertise, battery storage concerns [6], and monitoring needs affect widespread adoption and efficiency. In this paper, a solar charging monitoring system has been developed using Arduino Uno to enhance the efficiency of lighting applications.

METHODS

The flow of the project involved solar energy generation, battery charging via a charge controller, and automated LED lighting controlled by an Arduino based on ambient light detection. Fig.1 illustrates a solar power system where the solar panel supplies energy, monitored by voltage and current sensors, to a solar charge controller. The



controller manages energy flow to charge the battery and power an LED light, ensuring efficient and regulated power delivery for energy storage and lighting. Fig. 2 shows an Arduino-based automatic lighting system. The Arduino Uno receives input from an LDR sensor module that detects ambient light levels. Based on the sensor data, it controls a relay module to switch the LED light on or off, while system status and readings are displayed on an LCD screen. Table 1 lists the solar panel's electrical specifications, including power output, voltage, current, and tolerance for performance variation.

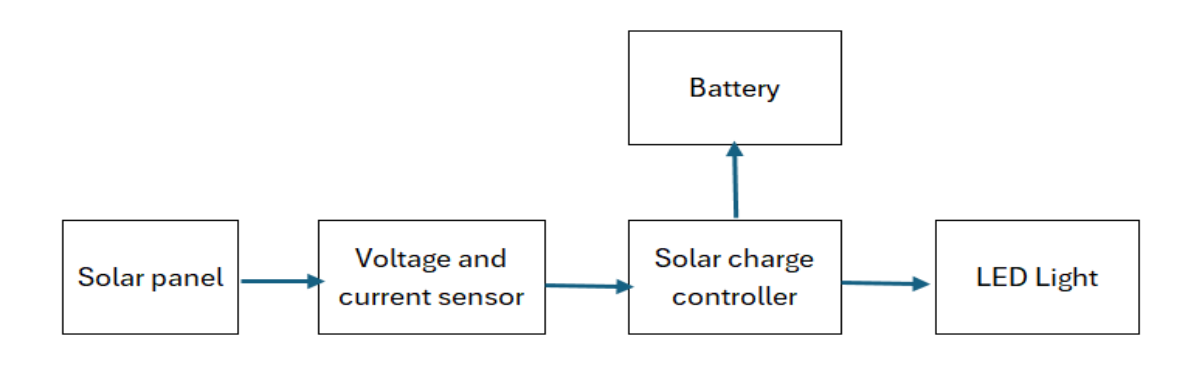


Fig 1. Solar system

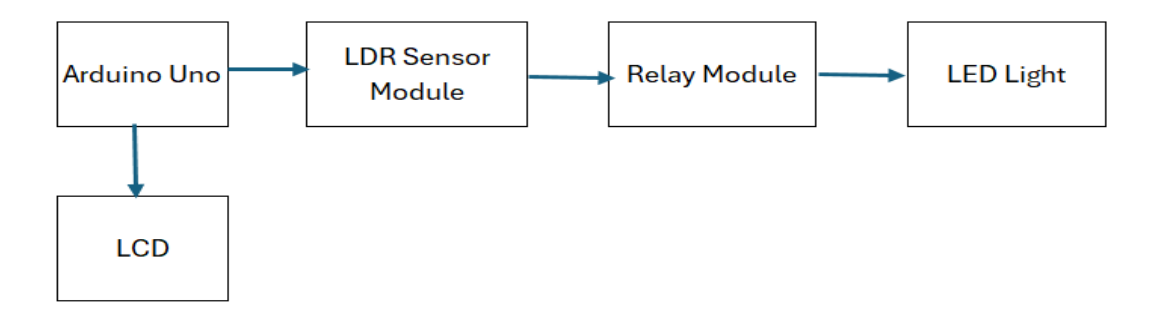


Fig 2. Lighting monitoring system

Table 2. Solar panel specification

Parameters	Value
Power Maximum	5W
Tolerance	+/- 5%
Vmp	12V
Imp	0.42A
Isc	0.45A

Fig. 3 shows a lighting monitoring system consisting of a solar panel, solar charge controller, 12V battery, and LED light. The system stores solar energy in the battery and powers the LED light, monitored via connected components for performance evaluation.



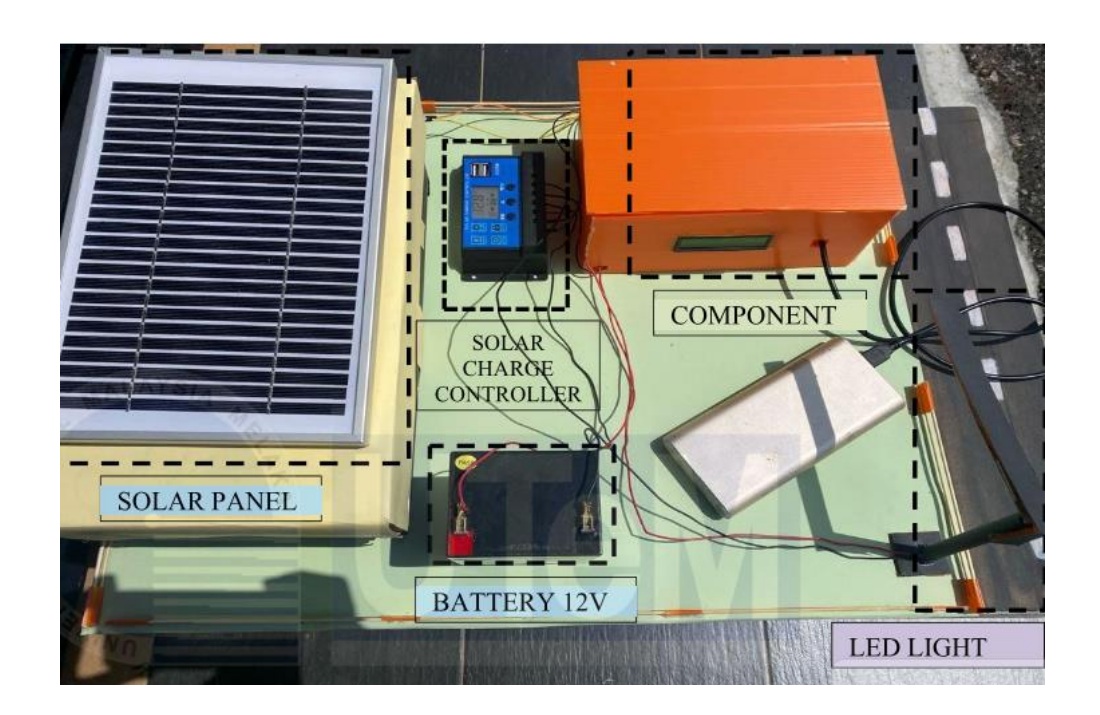


Fig 3. Lighting monitoring system

RESULTS AND DISCUSSION

As shown in Fig. 4, the solar panel voltage increases from 13.16 V at 8:00 a.m. to a peak of 13.98 V at 4:00 p.m., then drops to 13.08 V by 6:00 p.m. In contrast, the full system voltage peaks earlier at 12.92 V (2:00 p.m.) and declines to 12.3 V by evening. This indicates energy losses due to internal inefficiencies and environmental factors. Fig. 5 further reveals that while the solar panel outputs up to 4.2 W at peak, the system only delivers 1.55 W. These results highlight the need for effective system design, load management, and control strategies to improve overall performance.

42



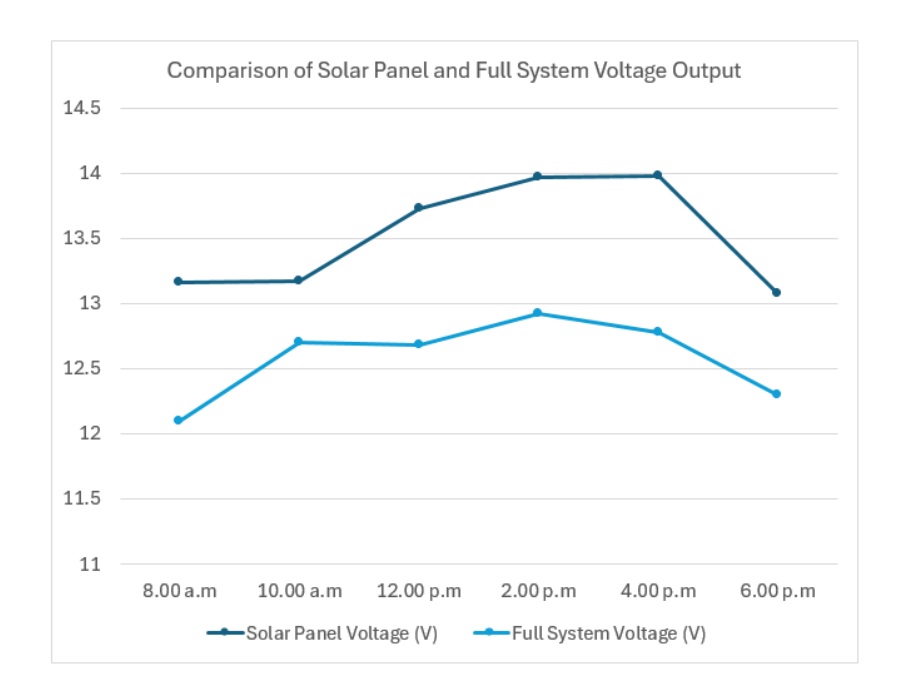


Fig 4. Comparison of Solar Panel and Full System Voltage Output

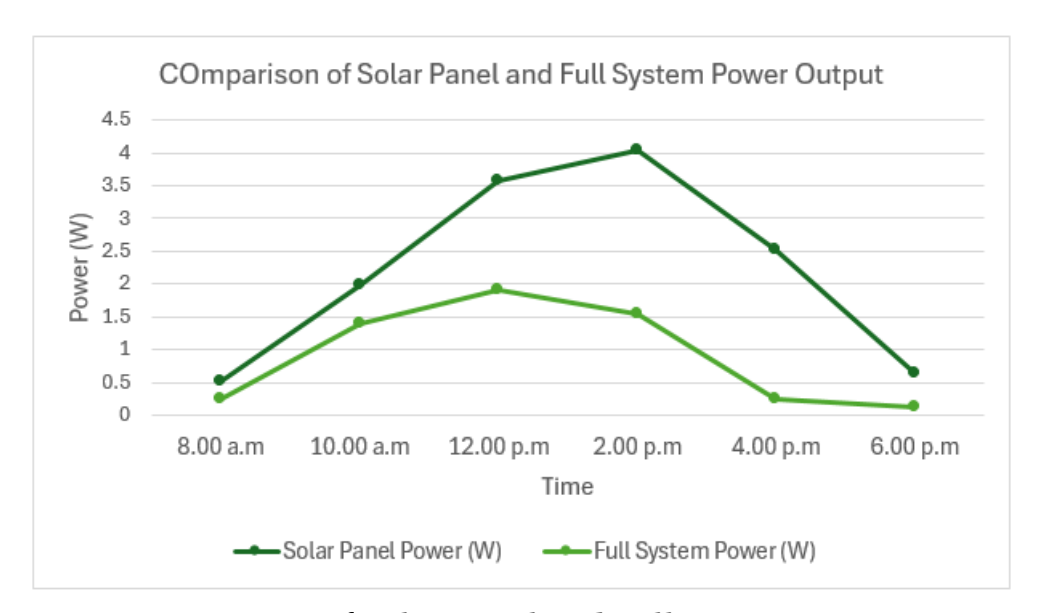


Fig 5. Comparison of Solar Panel and Full System Power Output

CONCLUSION

The solar charging monitoring system successfully demonstrates the integration of Arduino Uno with renewable energy components for efficient lighting control. Despite energy losses, the system provides an automated, sustainable solution for off-grid lighting needs. Future improvements in load management and energy storage can further enhance its performance and reliability.

ACKNOWLEDGMENT

The author(s) would like to thank Fakulti Teknologi dan Kejuruteraan Elektrik for the



support and resources provided for this research. Appreciation is also extended to all individuals who contributed to the success of this study.

REFERENCES

- [1] P. Zare, H. Ghadimi, R. Zare, A. B. Bork Abad, B. Sabery, and I. F. Davoudkhani, "The Study Impact of Restructuring on Efficiency of Iran's Electricity Distribution and Transmission Network," in 2023 8th International Conference on Technology and Energy Management, ICTEM 2023, Institute of Electrical and Electronics Engineers Inc., 2023. doi: 10.1109/ICTEM56862.2023.10083558.
- [2] S. F. Hui, H. F. Ho, W. W. Chan, K. W. Chan, W. C. Lo, and K. W. E. Cheng, "Floating Solar Cell Power Generation, Power Flow Design and its Connection and Distribution."
- [3] M. I. Fahmi, Hidayatullah, J. E. Hutagalung, and S. Sembiring, "Electrical automation of solar cellbased Arduino Uno with 16×2 LCD display," in Emerald Reach Proceedings Series, vol. 1, Emerald Group Holdings Ltd., 2018, pp. 629–639. doi: 10.1108/978-1-78756-793-1-00099.
- [4] T. M. Belay and S. M. Atnaw, "CFD Simulations and Experimental Investigation of a Flat-Plate Solar Air Heater at Different Positions of Inlet and Outlet," Journal of Renewable Energy, vol. 2023, pp. 1–16, Oct. 2023, doi: 10.1155/2023/3911228.
- [5] Q. Mu et al., "Research on power prediction of clean energy and operation optimization of clean energy supply system for typical regions," in 2023 3rd International Conference on Neural Networks, Information and Communication Engineering, NNICE 2023, Institute of Electrical and Electronics Engineers Inc., 2023, pp. 745–750.
- [6] H. Liu, B. Wu, A. Maleki, F. Pourfayaz, and R. Ghasempour, "Effects of Reliability Index on Optimal Configuration of Hybrid Solar/Battery Energy System by Optimization Approach: A Case Study," International Journal of Photoenergy, vol. 2021, 2021.



FAKULTI TEKNOLOGI DAN KEJURUTERAAN ELEKTRIK UNIVERSITI TEKNIKAL MALAYSIA MELAKA HANG TUAH JAYA, 76100 DURIAN TUNGGAL, MELAKA, MALAYSIA



ftke@utem.edu.my



+606-270 2112



+606-270 1044